

Air Force Institute of Technology

AFIT Scholar

Theses and Dissertations

Student Graduate Works

3-19-2009

Characterization of Hardening by Design Techniques on Commercial, Small Feature Sized Field-Programmable Gate Arrays

Thomas E. Simmons

Follow this and additional works at: <https://scholar.afit.edu/etd>



Part of the [Electrical and Electronics Commons](#), and the [Power and Energy Commons](#)

Recommended Citation

Simmons, Thomas E., "Characterization of Hardening by Design Techniques on Commercial, Small Feature Sized Field-Programmable Gate Arrays" (2009). *Theses and Dissertations*. 2564.
<https://scholar.afit.edu/etd/2564>

This Thesis is brought to you for free and open access by the Student Graduate Works at AFIT Scholar. It has been accepted for inclusion in Theses and Dissertations by an authorized administrator of AFIT Scholar. For more information, please contact richard.mansfield@afit.edu.



**CHARACTERIZATION OF HARDENING BY DESIGN TECHNIQUES ON COMMERCIAL,
SMALL FEATURE SIZED FIELD-PROGRAMMABLE GATE ARRAYS
THESIS**

Thomas E. Simmons, Captain, USAF

AFIT/GE/ENG/09-43

DEPARTMENT OF THE AIR FORCE

AIR UNIVERSITY

AIR FORCE INSTITUTE OF TECHNOLOGY

Wright-Patterson Air Force Base, Ohio

APPROVED FOR PUBLIC RELEASE; DISTRIBUTION UNLIMITED

The views expressed in this thesis are those of the author and do not reflect the official policy or position of the United States Air Force, Department of Defense, or the U.S. Government.

AFIT/GE/ENG/09-43

**CHARACTERIZATION OF HARDENING BY DESIGN TECHNIQUES ON
COMMERCIAL, SMALL FEATURE SIZED FIELD-PROGRAMMABLE GATE
ARRAYS**

THESIS

Presented to the Faculty

Department of Electrical and Computer Engineering

Graduate School of Engineering and Management

Air Force Institute of Technology

Air University

Air Education and Training Command

In Partial Fulfillment of the Requirements for the
Degree of Master of Science in Electrical Engineering

Thomas E. Simmons, BS

Captain, USAF

March 2009


APPROVED FOR PUBLIC RELEASE; DISTRIBUTION UNLIMITED

**CHARACTERIZATION OF HARDENING BY DESIGN TECHNIQUES ON
COMMERCIAL, SMALL FEATURE SIZED FIELD-PROGRAMMABLE GATE
ARRAYS**

Thomas E. Simmons, BS

Captain, USAF

Approved:



Yong Kim, PhD, USAF (Chairman)

19 MAR 09

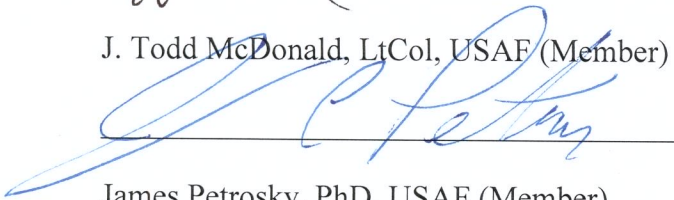
Date



J. Todd McDonald, LtCol, USAF (Member)

19 MAR 09

Date



James Petrosky, PhD, USAF (Member)

19 MAR 09

Date

Abstract

In this thesis, a methodology is developed to experimentally test and evaluate a programmable logic device under gamma irradiation. The purpose of which is to determine the radiation effects and characterize the improvements of various hardening by design techniques. The techniques analyzed in this thesis include Error Correction Coding (ECC) and Triple Modular Redundancy (TMR).

The TMR circuit includes three different functional implementations of adders compared to TMR voted circuits of those same adders. The TMR is implemented with the same functional adders and as a Functional TMR (FTMR) with three different function adders that are voted on. The three functional adders are: a behavioral adder that allows the FPGA synthesis software to create the implementation, a ripple carry adder that consists of multiple single bit full adders linked together, and a carry look ahead adder that operates the fastest by using an algorithm that creates generate and propagate signals. These adders are connected to single voter TMR and FTMR circuits to evaluate the improvements that could be obtained.

The ECC circuit includes Block RAM (BRAM) and Distributed RAM memory elements that are loaded both with ECC and non-error corrected data. The circuit is designed to check for errors in memory data, stuck bit values in the memory, and the performance improvements that ECC provides the system.

The results show that TMR or FTMR circuits failed at a rate at or above the single copy adders. This results from the single point of failure created by the voting logic being in the radiation environment. However, when the TMR or FTMR circuit is moved off-chip, the TMR single point of failure is removed and the results demonstrate much lower SEU error rates.

Acknowledgments

This document and my entire time at AFIT could not be possible alone and I want to thank those most important in helping me complete this journey. To my friends and colleagues, who have provided the much needed stress relief and support over the course of my time at AFIT. To my fellow VLSI graduate students, who helped me both in coding and analysis. To my family, their support has allowed me to achieve goals throughout my life. To the Ohio State Reactor team, their flexibility and knowledge allowed me to complete these experiments. And finally to Dr. Kim, who spent countless hours, day and night, to help me achieve this goal.

Tom Simmons

Table of Contents

ABSTRACT.....	V
ACKNOWLEDGMENTS	VII
TABLE OF CONTENTS.....	VIII
LIST OF TABLES	XIII
LIST OF ACRONYMS/ABBREVIATIONS	XIV
I. INTRODUCTION	1
1.1 CHAPTER OVERVIEW	1
1.2 MOTIVATION.....	1
1.3 PROBLEM STATEMENT	2
1.4 CONTRIBUTIONS	3
1.5 SEQUENCE OF PRESENTATION	3
II. LITERATURE REVIEW.....	5
2.1 CHAPTER OVERVIEW	5
2.2 BASIC RADIATION EFFECTS ON ELECTRONICS	5
2.2.1 Definitions.....	5
2.2.2 Radiation Source	6
2.2.3 Ionizing Radiation Effects on Electronics	8
2.3 FIELD PROGRAMMABLE GATE ARRAYS	10
2.4 RELATED WORK.....	11

2.4.1 Hardening by Design Research and Simulations	12
2.4.2 FPGA Radiation Analysis	13
2.5 CHAPTER SUMMARY	14
III. METHODOLOGY	15
3.1 CHAPTER OVERVIEW	15
3.2 DESIGN	15
3.2.1 Redundant Circuits with Voting	15
3.2.2 Error Detection and Correction Coding	17
3.3 EXPERIMENT	18
3.4 TEST PLAN	34
3.5 METHODOLOGY SUMMARY	36
4.1 CHAPTER OVERVIEW	38
4.2 RADIATIONS SUMMARY	38
4.3 CURRENT DRAW	41
4.4 FTMR/ADDER ERROR RESULTS	44
4.6 RESULTS SUMMARY	47
V. CONCLUSIONS	49
5.1 OVERVIEW	49
5.2 CONCLUSION STATEMENT	49
5.3 APPLICATIONS	49
5.4 FUTURE WORK	50

BIBLIOGRAPHY	51
APPENDIX A	53
APPENDIX B	53
APPENDIX C	53
APPENDIX D	53

List of Figures

FIGURE 2.1: CO-60 DECAY EMITTING 1 ELECTRON AND 2 GAMMAS	7
FIGURE 2.2: CO-60 GAMMA IRRADIATOR LAYOUT	7
FIGURE 2.3: DOSE RATE OF CO-60 IRRADIATOR	8
FIGURE 2.4: RESULT OF IONIZING RADIATION	9
FIGURE 2.5: BASIC 6 TRANSISTOR SRAM STRUCTURE IN FPGA	11
FIGURE 3.1: SIMPLE TRIPLE MODULAR REDUNDANCY VOTER	16
FIGURE 3.2: SINGLE BIT OF LUT VS. BUFFERED TMR VOTER.....	17
FIGURE 3.3: DUT VIRTEX 4 MINI-MODULE.....	19
FIGURE 3.4: HARDWARE SETUP	21
FIGURE 3.5: PICTURE OF HARDWARE SETUP	21
FIGURE 3.6: VIRTEX 5 ML505/6 CONTROL BOARD	22
FIGURE 3.7: BREAKOUT BOX CONNECTING TO CONTROLLER BOARD.....	23
FIGURE 3.8: CLOCK PIN TRANSMISSION FROM DUT TO CONTROL BOARD	24
FIGURE 3.9: DATA SYNCHRONIZATION WITH CLOCK.....	25
FIGURE 3.10: VIRTEX 4 FPGA FTMR/ADDER STRUCTURE.....	27
FIGURE 3.11: VIRTEX 4 FPGA TMR/FTMR STRUCTURE.....	27
FIGURE 3.12: VIRTEX 5 FPGA FTMR/TMR/ADDER ANALYSIS STRUCTURE	28
FIGURE 3.13: RIPPLE CARRY ADDER STRUCTURE.....	29
FIGURE 3.14: CARRY LOOK AHEAD ADDER STRUCTURE.....	29
FIGURE 3.15: 1ST BIT OF RC ADDER.....	30

FIGURE 3.16: 1ST BIT OF BEHAVIORAL ADDER	30
FIGURE 3.17: 1ST BIT OF CARRY LOOK AHEAD ADDER	30
FIGURE 3.18: VIRTEX 4 FPGA MEMORY STRUCTURE	32
FIGURE 3.19: VIRTEX 5 MEMORY ANALYSIS STRUCTURE	33
FIGURE 4.20: RADIATIONS 1-8: SHOWS KRAD(SI)/HR VS. POSITION IN TUBE	39
FIGURE 4.21: FPGA SUPPLY CURRENT VS. TIME AT 35 KRAD (SI)/HR	42
FIGURE 4.22: SUPPLY CURRENT VS TIME AT 50 KRAD (SI)/HR AND 67 KRAD (SI)/HR	43
FIGURE 4.23: ERRORS ON RADIATION #4 67KRAD (SI)/HR	46
FIGURE 4.24: ERROR ON RADIATION #5 35 KRAD (SI)/HR	46
FIGURE 4.25: ERRORS ON RADIATION#6 50 KRAD (SI)/HR	47

List of Tables

TABLE 2.1: TMR SIMULATION RESULTS	13
TABLE 3.1: UTILIZATION OF SEVERAL FUNCTIONAL UNITS	28
TABLE 3.2: MEMORY STRUCTURE ADDRESSES	34
TABLE 3.3: TMR DATA COLLECTION FORMAT.....	36
TABLE 4.4: SINGLE ADDER VS. SINGLE FTMR ERRORS	44
TABLE 4.5: TMR VS. FTMR ERRORS	45

List of Acronyms/Abbreviations

ASIC	Application Specific Integrated Circuit
BRAM	Block Ram
CMOS	Complementary Metal Oxide Semiconductor
Co	Cobalt
CPU	Central Processing Unit
DUT	Device-Under-Test
ECC	Error Correction Code
EDAC	Error Detection and Correction
EHP	Electron-Hole Pair
FPGA	Field Programmable Gate Array
FTMR	Functional Triple Modular Redundancy
IC	Integrated Circuit
IP	Intellectual Property
ISE	Integrated Synthesis Environment
LED	Light Emitting Diode
LET	Linear Energy Transfer
MBU	Multiple Bit Upset
MOS	Metal Oxide Semiconductor
MOSFET	Metal Oxide Semiconductor Field Effect Transistor
NMOS	MOSFET with an n-channel
NRL	Nuclear Research Lab
NVM	Non-Volatile Memory
OSU	Ohio State University
PMOS	MOSFET with a p-channel
RAM	Random Access Memory
SAF	Stuck-At-Faults
SEB	Single Event Burnout
SEE	Single Event Effect
SEGR	Single Event Gate Rapture
SEL	Single Event Latchup
SET	Single Event Transient
SEU	Single Event Upset
Si	Silicon
SiO ₂	Silicon Dioxide
SRAM	Static Random Access Memory
TID	Total Ionizing Dose
TMR	Triple Modular Redundancy
UART	Universal Asynchronous Receiver/Transmitter
USB	Universal Serial Bus
VHDL	VHSIC Hardware Description Language

VHSIC	Very-High-Speed Integrated Circuits
XPS	Xilinx Platform Studio
γ -ray	Gamma-ray

CHARACTERIZATION OF HARDENING BY DESIGN TECHNIQUES ON COMMERCIAL, SMALL FEATURE SIZED FIELD-PROGRAMMABLE GATE ARRAYS

I. Introduction

1.1 Chapter Overview

This chapter covers the following topics:

1. Motivation
2. Problem Statement
3. Plan of Attack
3. Contributions
4. Sequence of Presentation

1.2 Motivation

Space and terrestrial radiation sources are known to cause errors and malfunctions in integrated circuit designs. These effects from subatomic particles and ionizing radiation on integrated circuits are referred to as Single Event Effects (SEE). These effects can cause sequential and combinational elements of the integrated circuit to change states or values. The traditional method of minimizing these effects in space environments is to use radiation hardened application specific integrated circuits and programmable logic devices. However, these devices often require large lead times and cost orders of magnitude more than non-radiation hardened devices. Therefore, various

organizations are investigating using commercially available circuits in these harsh environments in order to reduce time and budget.

1.3 Problem Statement

State of the art systems are increasingly being developed on Field Programmable Gate Arrays (FPGAs), due to their cost and schedule performance benefits over traditional Application Specific Integrated Circuits (ASICs). However, with newer FPGAs with design features at 90nm and below, radiation effects in both space and some terrestrial environments limit the effective use of FPGAs. These effects often lead to the use of radiation hardened devices to limit these harmful effects.

Various designs work to make FPGAs less susceptible to radiation and offer increased reliability over standard FPGA designs. These design processes are called hardening by design. The objective of this work is to characterize these improvements so that these designs can be used in non-critical space applications that traditionally require radiation hardened FPGAs. Thus, the experimental design:

1. Evaluates the radiation effects on various hardened designs
2. Allows for analysis of failures
3. Allows for characterization of hardening by design techniques versus traditional non-hardened designs

The specific goal of this research is to evaluate and characterize hardening by design techniques on 90nm FPGA circuits. This facilitates replacement of physically

hardened ASIC and FPGAs, as well as allow for improvements in designs of non-radiation hardened electronics.

This research shows whether design hardening techniques such as Triple Modular Redundancy (TMR), Functional Triple Modular Redundancy (FTMR) and Error Correction Coding (ECC) can reduce system vulnerability to ionizing radiation.

1.4 Contributions

This thesis explores the effects of gamma radiation on different FPGA programming styles in an attempt to mitigate these effects on non radiation hardened FPGAs. The contributions of this work include an analysis of commercial off the shelf reconfigurable electronics in radiation environments. This is superior to the current use of radiation hardened devices in space environments. The contributions of this work include:

1. Successful design of a system for sending, receiving and analyzing data from an FPGA device under radiation.
2. Characterization of design hardening techniques versus standard FPGA programming. Design hardening techniques include TMR, FTMR and ECC.
3. An evaluation of design hardening techniques tested, including error locations, causes, and performance improvements.

1.5 Sequence of Presentation

The remainder of this thesis is divided in to five chapters followed by supporting appendices. Chapter 1 provides motivation, a basic problem statement, a plan of attack,

and contributions. Chapter 2 provides background information relevant to developing radiation hardened design. Chapter 3 covers the methodology used to design and test the radiation hardened design. Chapter 4 covers results of the characterization of the design improvements and Chapter 5 provides conclusions and discussion on future work. The appendices contain information considered too lengthy to include in the main body of the text but which provide additional information for those interested parties. This information includes the wiring setup, software code used for testing, and the raw data obtained from the irradiations.

II. Literature Review

2.1 Chapter Overview

This chapter covers:

1. Basic Radiation Effects on Electronics
2. Field Programmable Gate Arrays
3. Related work

2.2 Basic Radiation Effects on Electronics

This section covers basic definitions, the radiation source for experimentation, and the effects of ionizing radiation on a circuit.

2.2.1 Definitions

Understanding radiation effects on electronics requires an understanding of a few basic terms (Radiation Effects & Analysis Home Page):

- Ionizing Radiation – Electromagnetic radiation that has enough energy to overcome the binding of electrons in atoms or molecules.
- Single Event Effect (SEE) - Any measurable effect to a circuit due to ion strikes.
- Single Event Transient (SET) – A voltage pulse through a circuit caused by ion strikes.
- Single Event Upset (SEU) - A change of state induced by an ionization damage to a circuit. SEUs are soft errors that a reset or rewriting of the device will cause normal device behavior.

- Multiple Bit Upset (MBU) - An event induced by a single energetic particle that causes multiple upsets or transients during its path through a device or system.
- Single Hard Error (SHE) - An SEU which causes a permanent change to the operation of a device. An example is a stuck bit in a memory device.
- Single Event Latchup (SEL) - A condition which causes loss of device functionality due to a single event induced high current state. An SEL may or may not cause permanent device damage, but requires power strobing of the device to resume normal device operations.
- Single Event Burnout (SEB) – A condition which can cause device destruction due to a high current state in a power transistor.
- Single Event Gate Rupture (SEGR) - A single ion induced condition in power transistors which may result in the formation of a conducting path in the gate oxide.

2.2.2 Radiation Source

The cobalt-60 isotope (Co-60) is used as the source of ionizing radiation for this experiment. Co-60 undergoes beta decay with a half-life of 5.24 years releasing two gamma particles and one electron, illustrated in Figure 2.1.

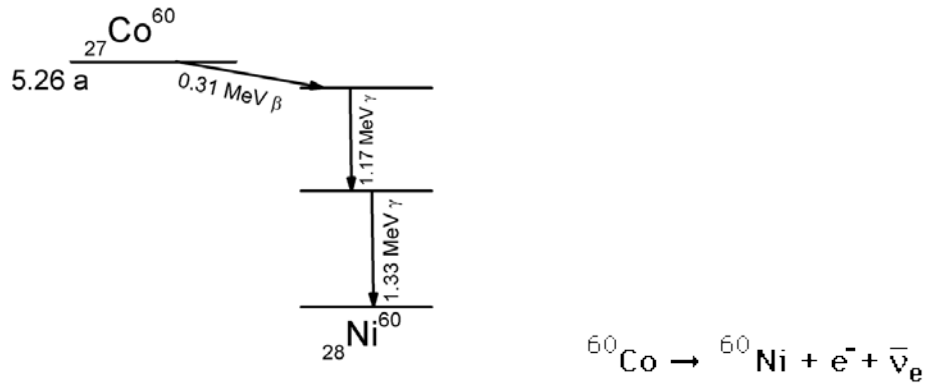


Figure 2.1: Co-60 Decay Emitting 1 Electron and 2 Gammas

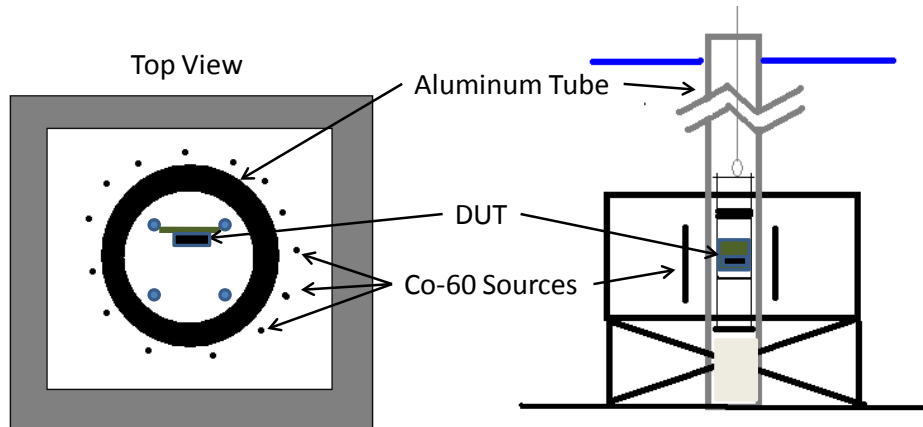


Figure 2.2: Co-60 Gamma Irradiator Layout

A Co-60 source is available at the Ohio State University(OSU) Nuclear Reactor Lab(NRL) in Columbus, Ohio. This gamma irradiator is shown in Figure 2.2. It contains a six inch wide aluminum tube containing a movable platform that can be raised and lowered out of the irradiator. The gamma irradiator cell itself sits on the bottom of a pool of water and consists of 14 Co-60 sources evenly spread around the aluminum tube.

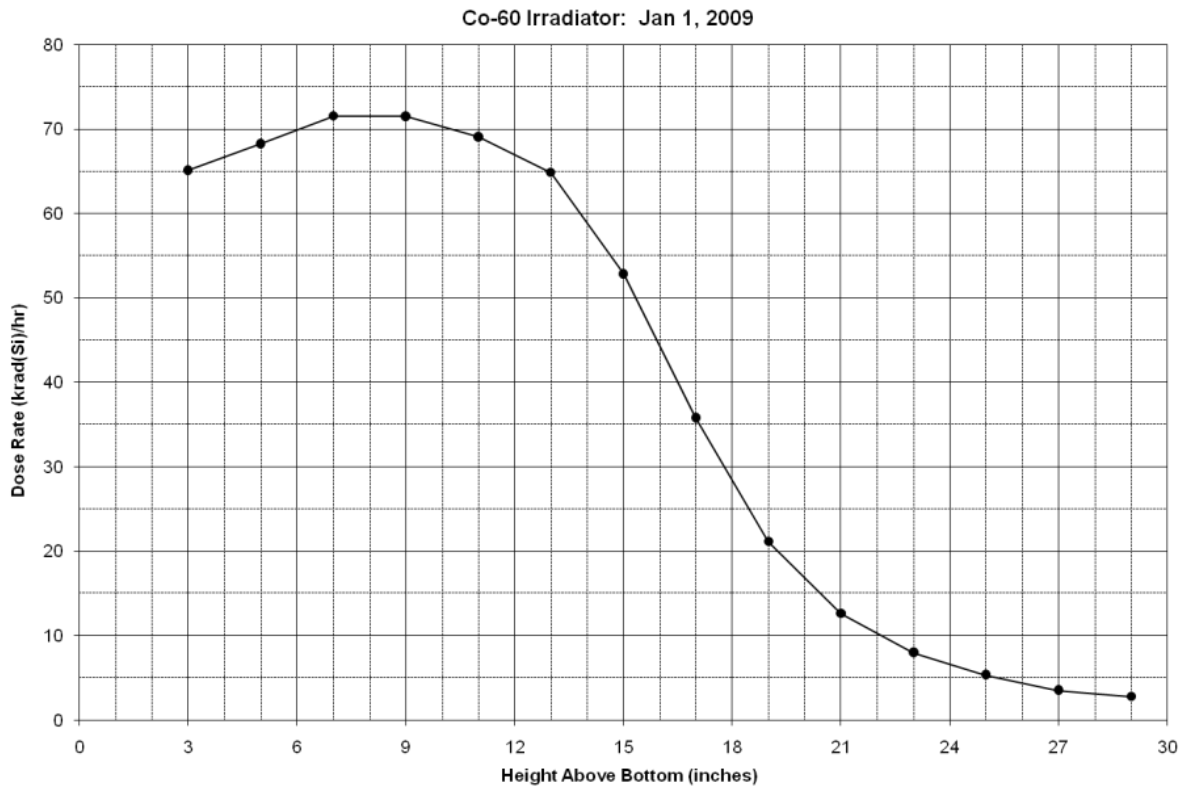


Figure 2.3: Dose Rate of Co-60 Irradiator (Herminghuysen)

When the device under test (DUT) is lowered into the tube, the radiation dose is based on the location of the device relative to the center of the Co-60 source rods. However, the dose curve is based on the distance of the DUT above the bottom of the moveable platform when the platform is resting on the bottom of the aluminum tube. An example radiation dose curve is depicted in Figure 2.3.

2.2.3 Ionizing Radiation Effects on Electronics

Ionizing Radiation creates electron hole pairs in materials by freeing electrons from the atoms or molecules that they are bonded to. When this occurs in electrically conductive materials, these electrons are free to quickly move back to lowest energy

states thus recombining the electrons with available holes almost instantly. However, in nonconductive materials, such as gate oxides in nmos transistors, the electron hole pairs take longer to recombine. The electrons, having a higher mobility than holes, are then drawn from the oxide leaving a positive charge in the oxide. When power is applied to the gate on nmos devices, these holes with a positive charge are pushed toward the gate interface with the substrate. This is a result of both the decrease in the distance between the gate charge and the substrate and the increased positive charge on the gate. In fact, if enough charge builds in the transistor's gate oxide the NMOS circuit can turn on without a charge applied to the gate input, effectively shorting the transistor. Figure 2.4 shows the transistor after irradiation.

According to hole-trapping models, hole-traps are formed transistor gate oxides. If there is a positive-bias applied to an n-channel CMOS device, electrons are quickly swept out of the oxide in less than a pico-second due to the higher mobility of electrons compared to holes. Some electrons will recombine with the holes. However, this varies depending on the electric field and the ionizing source. The holes are relatively immobile compared to the electrons and can cause a temporary negative threshold voltage shift.

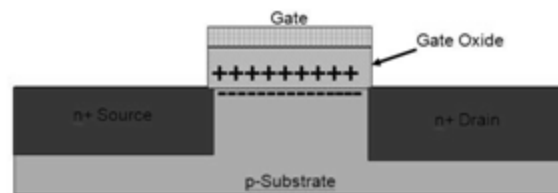


Figure 2.4: Result of Ionizing Radiation: Formation of a Shorting Path between the Source and Drain of NMOS Transistor (Arnold)

Depending on the applied electric field, the temperature, oxide thickness, and fabrication techniques the holes will slowly migrate toward the oxide-substrate interface by polaron hopping (Petrosky; Rollins, Wirthlin and Graham)

2.3 Field Programmable Gate Arrays

Field Programmable Gate Arrays (FPGAs) are a type of circuit that is programmed in the field rather than in a semiconductor fabrication. It consists of programmable interconnects in the circuit that allow the connection of various gates and structures. These interconnects require a large amount of FPGA area resulting in a chip with very low gate density compared to Application Specific Integrated Circuits (ASICs.) The vast majority of FPGAs are SRAM-based, although there are some flash and antifuse versions. Typically, the antifuse varieties are of interest to aerospace designers because they are more radiation hardened. However, their increased costs reduce the advantages of using FPGA over ASICs. Therefore, more and more often designers are looking to use non-hardened SRAM FPGAs in place of these design hardened devices.

FPGAs are currently manufactured by several manufacturers with Xilinx and Altera dominating the market. Each manufacturer also has their own unique computer based programming tools for use with their specific FPGAs. The Xilinx package of various FPGA development tools is the Integrated Synthesis Environment (ISE) Design Suite. This suite includes many tools with two main programming environments - ISE Foundation and Xilinx Platform Studio (XPS). The ISE tool is used primarily for Very-High-Speed Integrated Circuits (VHSIC) Hardware Design Language (VHDL) implementations. The XPS tool is used for implementing Intellectual Property (IP) cores

such as embedded processor designs like the MicroBlaze soft core and PowerPC microprocessors. ISE VHDL projects can be implemented as IP cores inside XPS to integration of user created cores into XPS software (Xilinx Inc)

SRAM based FPGAs consist of control logic routing the devices in the FPGA fabric together. An example of the SRAM cell that is the basic structure that makes up the FPGA is shown in Figure 2.5.

2.4 Related Work

Two main organizations that are heavily involved in radiation effects research are Los Alamos National Laboratories and NASA Goddard Space Flight Center. They are two key players in radiation effects on circuits. Therefore, many of the papers in this section come from their research and research that they support in this field.

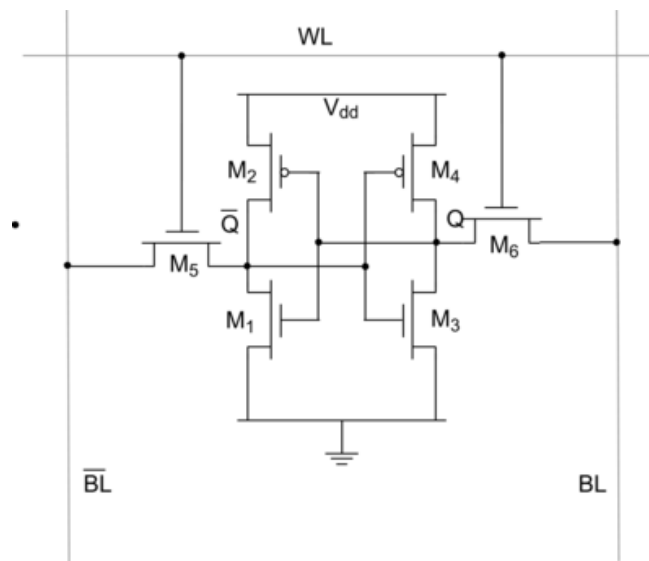


Figure 2.5: Basic 6 Transistor SRAM Structure in FPGA

2.4.1 Hardening by Design Research and Simulations

Significant research exists on hardening by design techniques. This predominantly includes fault injection analysis of various hardened designs. Previous work ranges from simple fault injection analysis of various TMR and Error Detection and Correction (EDAC) designs to proposals for more advanced design hardening techniques.

An example of TMR fault injection shows TMR voting on incrementer and counters designs. Counter intuitively, the results show the single voter TMR can produce results as bad as or worse than a single version of a counter without redundancy. This is a result of the single point of failure inherent in the TMR design (Rollins, Wirthlin and Graham). Table 2.1 shows the results of fault injection on four different TMR designs. This single point of failure can be fixed by various techniques including using feedback, final TMR voting off chip, or utilizing check voters which validate the results of the majority TMR voters (Rollins, Wirthlin and Graham). Additionally, research demonstrates various EDAC techniques including ECC and more advanced techniques. One useful technique on FPGAs is called Lightweight EDAC (LEDAC). LEDAC implements array based code compared to traditional word or line encoding schemes. This allows for much greater error detection and correction than

Table 2.1: TMR Simulation Results (**Rollins, Wirthlin and Graham**)

Design (single clock)	Simple Incrementer			Up/Down Loadable Counter		
	LUTs	Failures	Speed (MHz)	LUTs	Failures	Speed (MHz)
No Redundancy	8	446	220	10	463	220
1 Voter	35 (~4x)	410	217 (99%)	41 (~4x)	484	217 (99%)
3 Voters	51 (~6x)	14	199 (91%)	57 (~6x)	14	213 (97%)
Feedback	51 (~6x)	14	160 (73%)	57 (~6x)	15	157 (72%)
Map Feedback	27 (~3x)	15	194 (88%)	N/A		

ECC with less overhead (Karl, Samson and Clark). This scheme is ideal for FPGAs due to their high level of multi-parallelism, meaning this EDAC could function with no existing FPGA hardware.

2.4.2 FPGA Radiation Analysis

Radiation testing of the newest radiation hardened and non-radiation hardened FPGAs are on-going for space and terrestrial applications. This research indicates that the primary SEUs occur in the logic memory of the SRAM FPGA. These papers demonstrate that configuration memory and Input/Output (I/O) pads are less likely to have SEUs effect the outputs of the FPGA since they require multiple bits to be changed in order for an error occur (Ceschia, Violante and Reorda). Additionally, dose ranges on radiation hardened devices are shown to meet the minimum radiation hardened standard of greater than 300 krad. Doses on non-radiation hardened devices are generally an order of magnitude lower (Brown and Brewer).

Single Event Upsets at ground level are also observed showing the need to add hardening by design techniques to some safety critical applications in terrestrial environments as well (Claeys and Simoen).

2.5 Chapter Summary

This chapter discusses relevant radiation effects on electronics, some basic FPGA information and a summary of some related research in the field of radiation effects of FPGAs and specifically hardening by design techniques.

III. Methodology

3.1 Chapter Overview

This chapter discusses the methodology for analysis of the hardening by radiation techniques. The materials covered in this chapter include the test design, the experimental setup, and the format of the data for analysis. The test design, covered in Section 3.2, describes the hardening by design techniques. Section 3.3 discusses how the hardware and software were designed for the experiment. Section 3.4 discusses the test plan including how the data is received for the radiation experiment and how that data is analyzed to produce results. Finally, Section 3.5 summarizes the Chapter.

3.2 Design

The design is setup to test the effects of Triple Modular Redundancy (TMR), Functional TMR (FTMR), and Error Correction Coding (ECC).

3.2.1 Redundant Circuits with Voting

There are several methods of voting on redundant logic or functionally redundant logic in order to reduce the effects of SEUs on the outputs of a logic module. The most common of these is the use of triple modular redundancy, shown in Figure 3.1, to mask faults. This technique triplicates all inputs and logic and passes the results to a bit-wise voter unit that takes the majority result to provide an output.

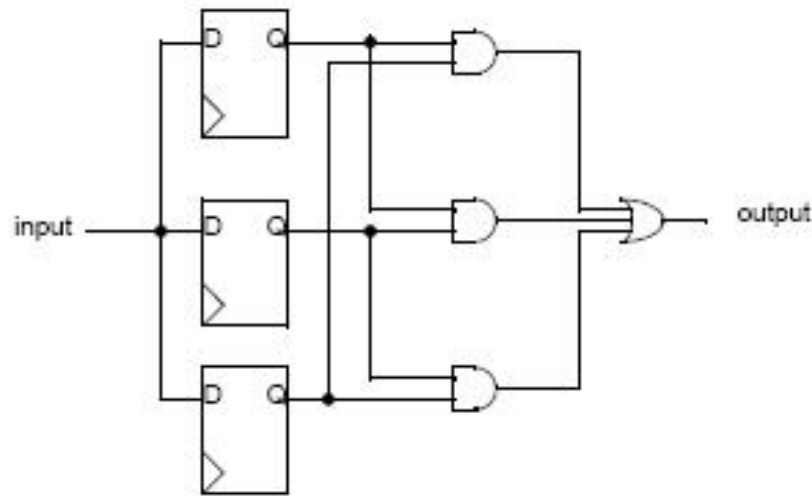


Figure 3.1 : Simple Triple Modular Redundancy Voter

Single voter TMR systems can result in a single point of failure. Thus, several techniques have been developed to mitigate the errors caused by the single point of failure in a TMR system. These techniques include three voter TMRs, word wise TMRs and buffered TMRs.

Three voter TMRs provide three separate copies of the outputs, which greatly reduces the errors from the single point of failure of a single voter system. This system is then eventually passed to a single voter for the final result. However, this step adds much less relative error than voting at each intermediate step.

Word-wise TMRs involve forcing the FPGA configuration to vote on the output value in multiple bit sections rather than bit by bit which is the default for voter logic. This word wise voting has been shown to decrease errors in simulations.

Another approach involves the use of buffer based TMRs which has been shown to reduce the SEU effects in the voter logic in simulations. An example of a buffer based TMR is shown in Figure 3.2.

The thesis analyzes the effects on single voter TMRs versus different functional implementations. Additionally, it investigates improvements possible by using a Functional TMR that takes a vote on three functional implementations instead of three copies of the same implementation. To show the improvements of triplicating TMR logic, the control board counts and outputs the results from each TMR for analysis of improvements of a final TMR that is placed off-chip. Due to constraints of the serial output to the PC, a total count of the control board TMR errors is used for analysis.

3.2.2 Error Detection and Correction Coding

There is a wide range of error detection and correction techniques that are used to protect memory data. These techniques range from simple error detection schemes, such as parity checks, to the more advanced error correcting code, some of which are currently used in memory systems. These error detection and correction techniques have

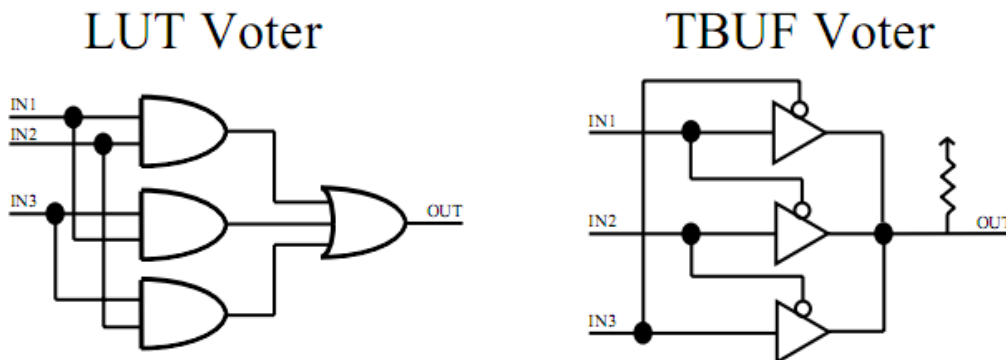


Figure 3.2: Single Bit of LUT vs. Buffered TMR Voter

additional data stored in memory in order to allow for error detection. Then if errors are detected, the data is corrected by either resending the data from its source or by including sufficient information in the data to allow it to correct itself.

One of the most common types of ECC memory involves the use of Hamming Code. Even though a single cosmic ray can upset many physically neighboring bits in a memory system, such memory systems are designed so that neighboring bits belong to different words, so that an SEU causes only a single error in any particular word, and can be corrected by a single-bit error correcting code. As long as not more than a single bit in any particular word is affected by an error between accesses, a memory system presents the illusion of an error-free memory. The Hamming Code is based additional memory spaces which store error correcting bits with every memory line. These error correcting bits allow for any single bit error to be corrected and any two bit error to be detected.

3.3 Experiment

This section summarizes the test framework including the DUT, the radiation experiment and the plan for the experiments run at the OSU reactor.

3.3.1 Device-Under-Test

The FPGA devices under test for these radiation experiments are Xilinx Virtex 4 Mini-modules mounted on an Avnet Mini-Module Baseboard, pictured below in Figure 3.3. The baseboard contains a socket for the two – 2 x 32 2mm FPGA headers to connect to multiple I/O interfaces and power supplies on the baseboard. The entire baseboard and FPGA Mini-Module combination is useful due to its dimensions being less than 4 by 6 inches, which is very suitable for this particular radiation experiment.

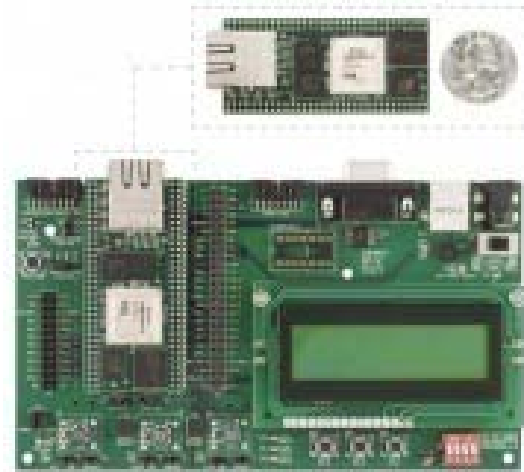


Figure 3.3: DUT Virtex 4 Mini-Module

Additional features of the Mini-module include autonomous operation without the baseboard, which could be extremely useful for additional experimental setups. The Xilinx Virtex 4 Mini-Module is designed as a complete system on a module. The Mini – Module packages all the necessary functions needed for an embedded FPGA onto a tiny footprint. The on-board MicroBlaze core provides processing capabilities, while the configurable I/O settings offer versatile interface options.

The FPGA contained on the mini-module is a Virtex 4 SC4VFX12, referred to as Virtex 4 FX12, FPGA. The Virtex 4 FX12 FPGA contains an array of 64 x 24 logic blocks supporting a maximum of 86 kilobits (Kb) of distributed memory plus the separate 80 Kilobytes (KB) (or 640 Kb) of block ram. The FPGA contains 90nm transistor technology with 10 layers of metal interconnects and triple oxide technology running internally at 1.2 Volts (V).

The distributed memory is contained in the logic slices of the FPGA and therefore consumes resources that could be used for other logic on the FPGA. The maximum width

of the distributed memories for the Virtex 4 is 1024, however, to maximize slice utilization smaller sizes are used and can be placed without causing routing problems when ISE places the logical slices on the FPGA. If larger memory sizes are needed, the block ram slices are generally more suitable as they are contained on separate slices that are only used for memory storage and therefore can be in a single memory structure as large as 80 KB (Xilinx Inc).

The triple oxide technology involves using three different gate oxide thicknesses in order to increase speed internally while still allowing the I/O at 3.3 V and the slower core logic containing the configuration data. The thick gate oxide is designed to withstand at least 3.6 V from the I/O transistor interface. The middle oxide or mid-ox thickness is for core logic that does not need to be fast and therefore the increased oxide thickness saves FPGA power. The main use of mid-ox is for the millions of transistors that store the configuration (six transistors for each configuration bit). Giving these transistors a thicker gate oxide reduces their leakage current substantially (Xilinx Inc).

3.3.2 Hardware setup

In addition to the DUT explained above, the hardware setup used to analyze the data from the DUT consists of the several parts. These parts include an ML506 FPGA board, two break-out boxes, two Fluke Multi-meters with data logging, a laptop computer, and associated wires. Additionally, Agilent Digital Logic Analyzers and Oscilloscopes are used in DUT design, analysis, and testing but not at the OSU irradiator. Figure 3.4 describes the hardware setup and Figure 3.5 shows the equipment connected in the lab.

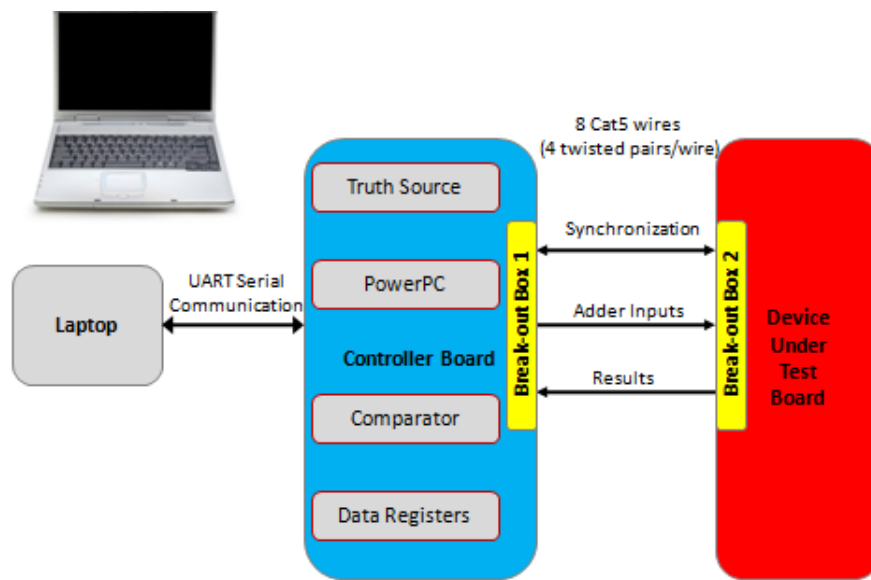


Figure 3.4: Hardware Setup

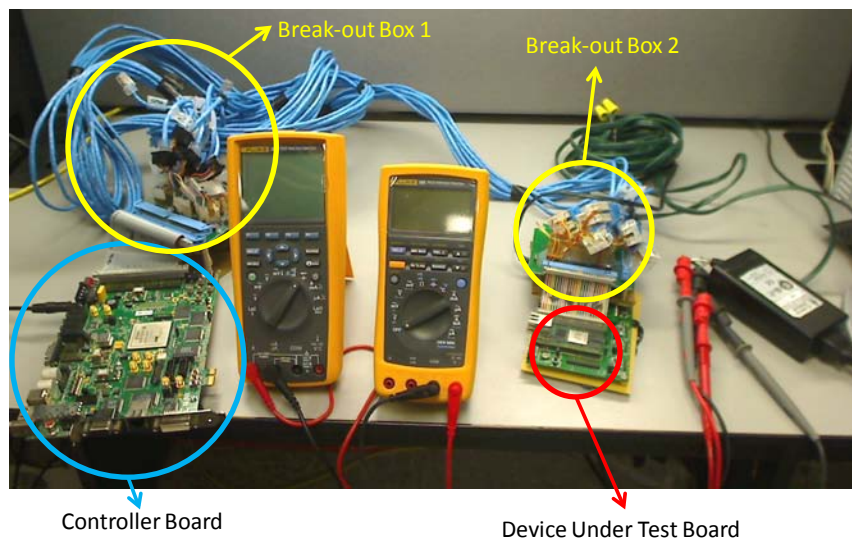


Figure 3.5: Picture of Hardware Setup



Figure 3.6: Virtex 5 ML505/6 Control Board

The ML506 FPGA board pictured in Figure 3.6 is utilized for analysis and display of results to the laptop computer. The specific board hardware used includes 32 singled I/O header connections, the FPGA, pushbuttons, serial port and LEDs. This board is utilized since it contains an FPGA with a built- in MicroBlaze microprocessor core, allowing for programming in C++ in addition to VHDL.

The breakout boxes consist of wiring to connect the single-ended inputs of the DUT and the control board, shown in Figure 3.7. Details of wiring attachments are contained in Appendix A. The breakout boxes utilize RJ45 jacks to connect eight 15' Cat5 Ethernet cables to the send data to and from the DUT.

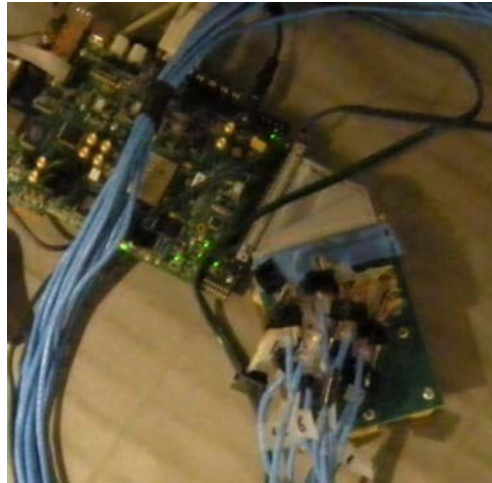


Figure 3.7: Breakout box connecting to Controller Board prior to Irradiation

These breakout boxes effectively transmit the single ends signals in excess of 15 ft. However, some noise and approximately 25 ns of signal delay occur during transmission. This results in signals synchronization issues during testing and which are remedied by the having individual signals sent on the positive edge of the clock not being read until the negative edge of the clock, approximately 150 ns after transmission of the data. An example of the clock signal at the DUT and control board I/Os is displayed in Figure 3.8.

The laptop for the programming the boards and collecting the data is a Dell Latitude D830. The laptop contains HyperTerminal software for communication with the MicroBlaze processor on the FPGA and Xilinx software necessary for programming the FPGA Boards.

In addition to the equipment used for the radiation testing, an Agilent Logic Analyzer is utilized to view the signals transmitted between the DUT and control board.

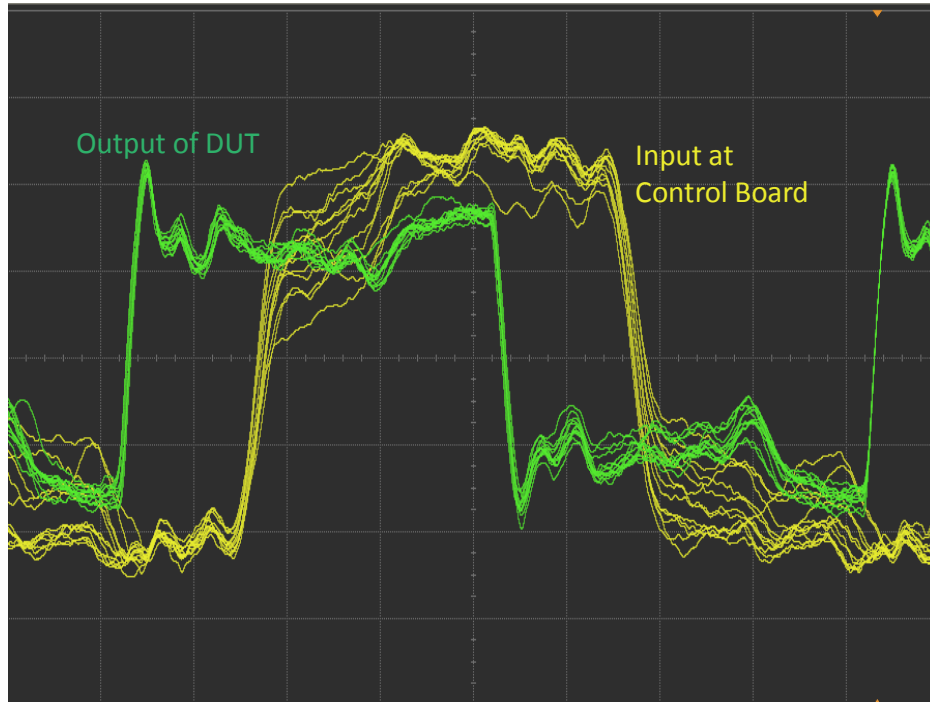


Figure 3.8: Clock Pin Transmission from DUT to Control Board (Scale: 20ns/ horizontal, 1V/ vertical)

This device allows analysis of data synchronization and functionality of the DUT both before and after the irradiations. An example of the data from the logic analyzer is shown in Figure 3.9. The figure shows how the data during the positive clock cycle is noisier.

3.3.4 Software Setup

Two separate software setups are made for the radiations tests with the software for both the DUT and the controller board programmed in VHDL utilizing Xilinx ISE software. However, the control board files are transferred over to Xilinx XPS as an IP core, such that the MicroBlaze microprocessor core can be utilized for display and analysis of results. The actual code utilized is on stored as Appendix B.

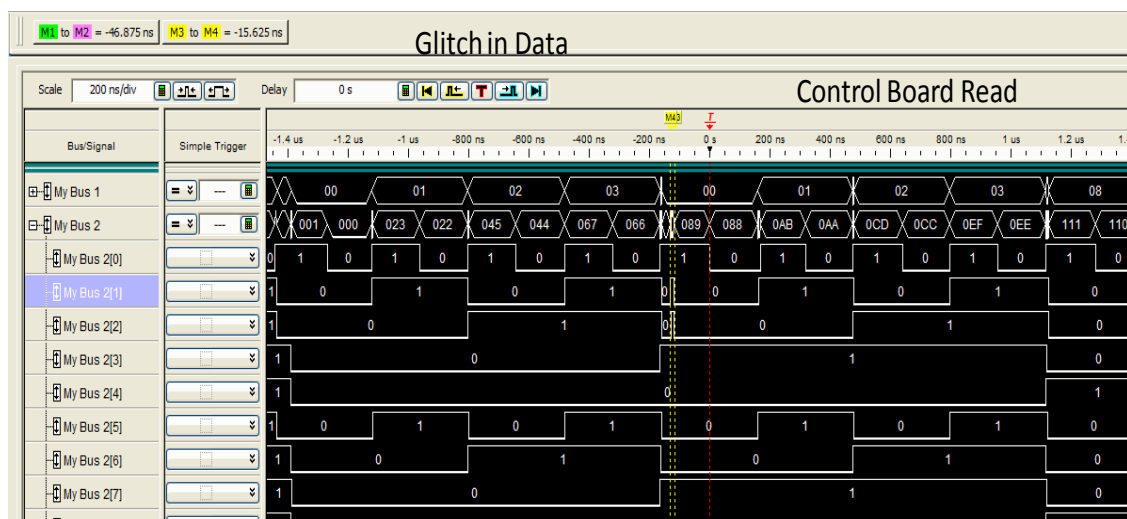


Figure 3.9: Data Synchronization with Clock

3.3.4.1 TMR Software Setup

The first software setup consists of DUT code to test triple modular redundancy versus the three different designs of adders. This code utilizes the 29 single ended I/Os on the DUT board to receive and to send out adder and TMR results at a frequency of at most 3.24MHz. The maximum frequency is determined by observing line delays and noise on the single-ended I/O lines. This indicates that the line has noise induced errors for up to 50 ns after transmission indicating the clock needs to be run at 10MHz or slower in order to capture data during the second half of the clock cycle. The system is tested with various frequency divisors based on the original 100MHz DUT clock. This resulted in a minimum frequency divisor to capture data without capturing erroneous data of 32. This indicates that the logic analyzer recognizes one and zero value transitions differently than the control board.

An illustration of the code with the three adders and the FTMR outputting data is shown in Figure 3.10. An illustration of the code used to compare different TMR structures with the FMTR structure is shown in Figure 3.11.

The FTMR/Adder DUT code is paired with controller board code that is built to compare the results to the truth source produced on the controller board and display the results through the UART connection to the PC containing HyperTerminal software. The comparator software operates at the same frequency as the DUT board clock and the comparator then outputs data to registers for display by the MicroBlaze processor. The processor operates at 235 MHz on the Virtex 5 board and analyzes and controls the display of data contained in the registers. The data is then displayed to the user via the RS232 Serial Communication IP Core running at 9600 bps. This means that if errors are occurring faster than can be displayed by the serial communication, the data is lost. Therefore, error totals are displayed in order to identify errors that are not displayed. This means that off-chip voting must be done real-time on the control board with running totals of errors since post analysis may not be possible if multiple errors occur. A diagram of this structure is shown in Figure 3.12.

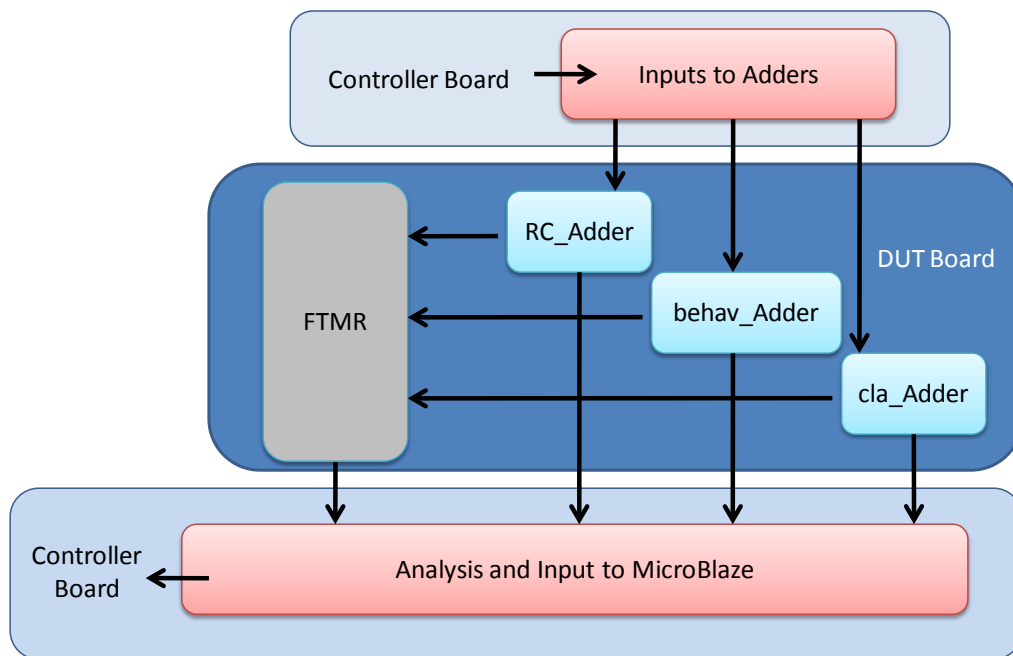


Figure 3.10: Virtex 4 FPGA FTMR/Adder Structure

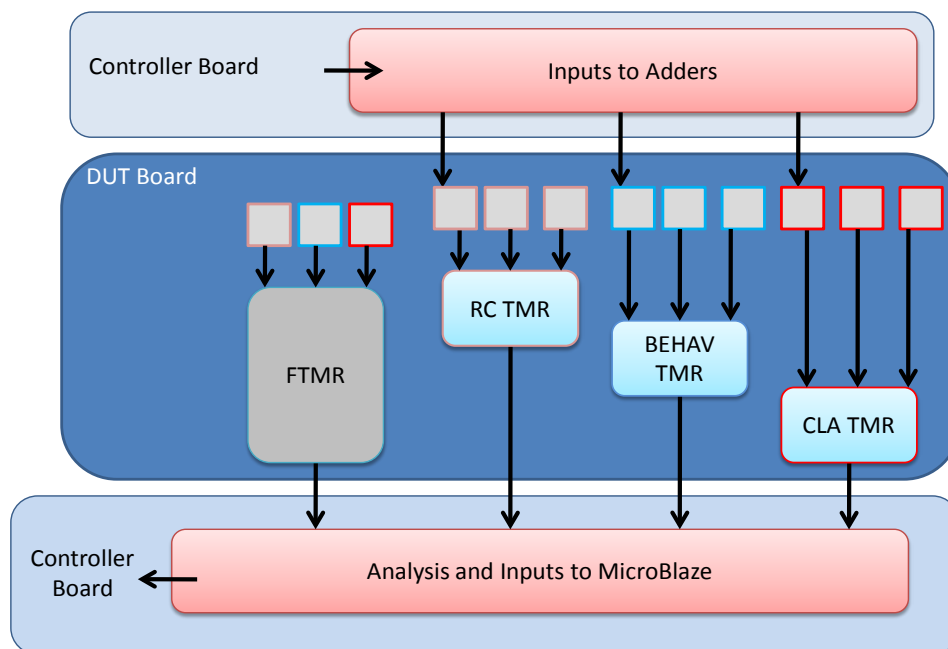


Figure 3.11: Virtex 4 FPGA TMR/FTMR Structure

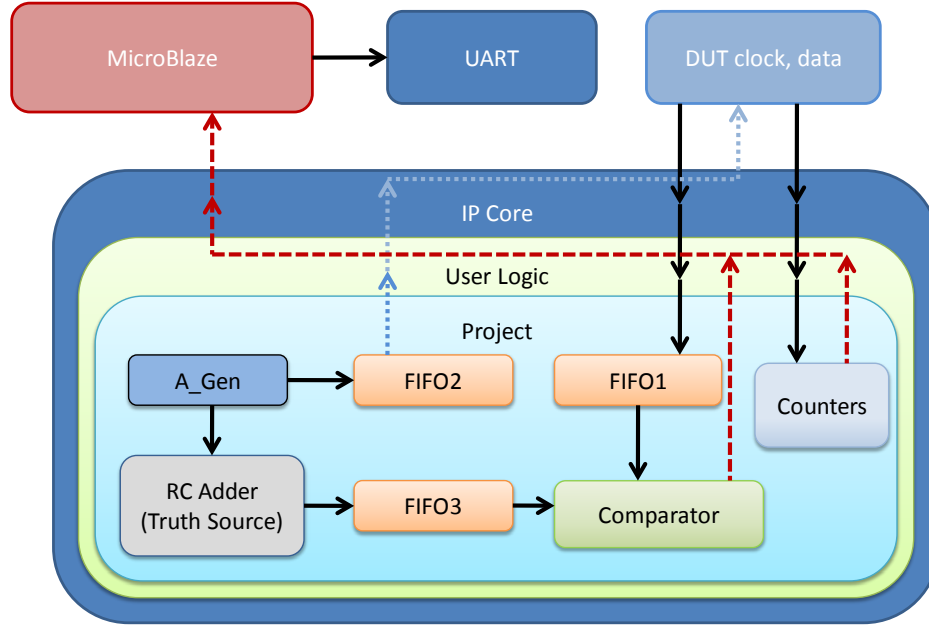


Figure 3.12: Virtex 5 FPGA FTMR/TMR/Adder Analysis Structure

The total resource allocation for each functional adder in comparison to the TMR structure is important to analyzing the potential radiation damage. The DUT utilization summary is contained in the Table 3.1. These numbers reflect the FPGA components used but do not reflect the actual structure of these components.

Table 3.1: Utilization of Several Functional Units

Module	slices	Slice Regs	LUTs
RC	3	4	3
Behav	4	4	12
CLA	3	4	3
FTMR	12	6	24

The designs of the ripple carry and carry look ahead adders are shown in Figures 3.13 and 3.14, where a and b are the adder inputs and S and C are the Sum and Carry outputs, respectively. The behavioral adder is not shown since it is created by the Xilinx synthesis tool and is essentially a black box with A and B inputs and S and C outputs.

The actual structures of the LUTs used for each structure can also be viewed through use of the ISE tools. The logic used for the first bits of each adder is shown in

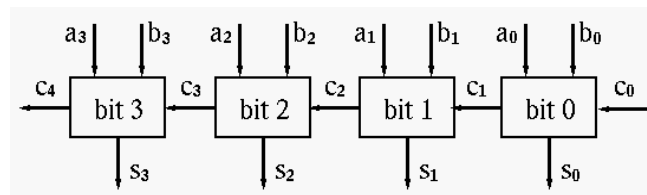


Figure 3.13: Ripple Carry Adder Structure

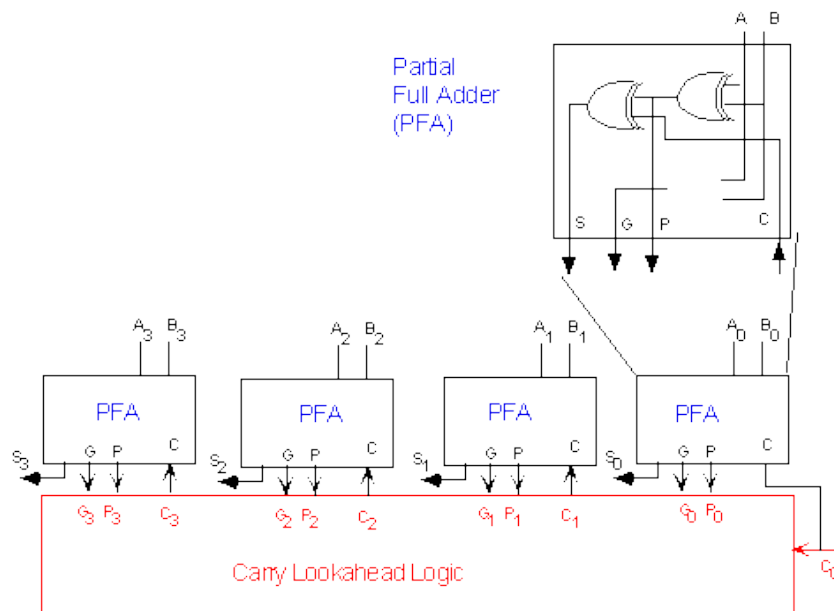


Figure 3.14: Carry Look Ahead Adder Structure

Figures 3.15, 3.16, and 3.17. These figures represent only a small section of the devices with the carry look ahead adder also having additional logic for the propagate and generate functions.

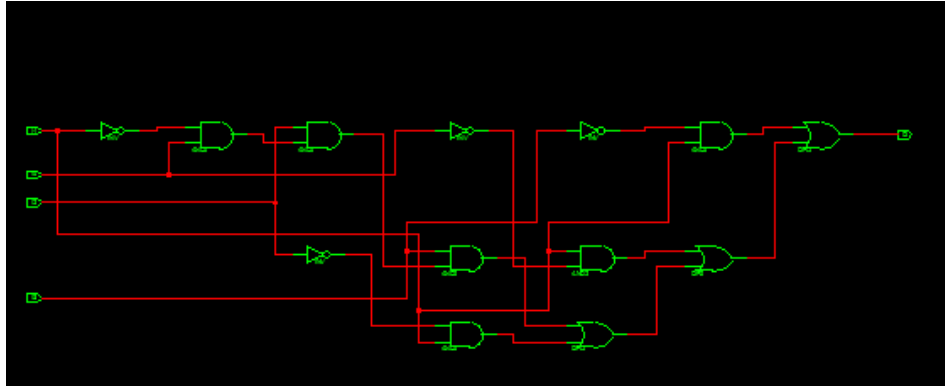


Figure 3.15: 1st Bit of RC Adder

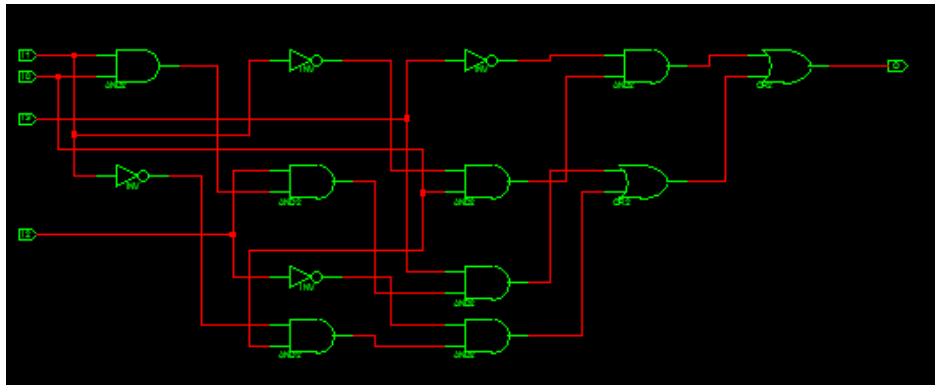


Figure 3.16: 1st Bit of Behavioral Adder

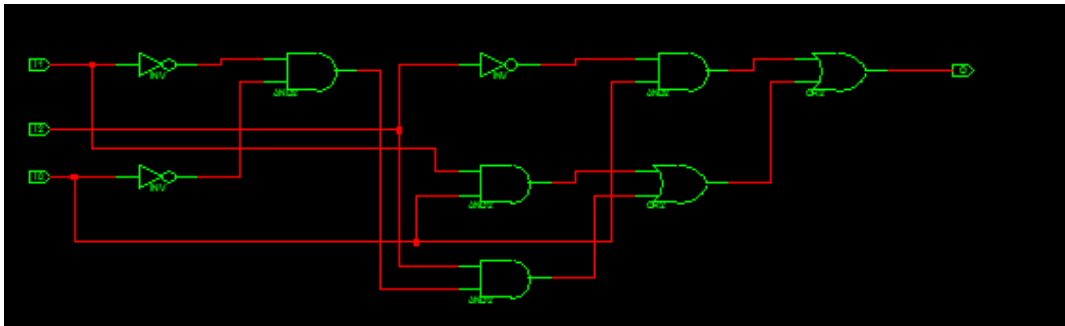


Figure 3.17: 1st Bit of Carry Look ahead Adder

3.3.4.2 ECC Memory Software Setup

The second software setup is built to test the radiation effects on the FPGA containing various memory structures. The four structures included 32 KB of block ram, 20 KB of BRAM with ECC, up to 8 KB of distributed memory, and up to 13 KB of distributed memory with ECC. These four structures are chosen since they maximize the available block ram, 80KB, and available distributed memory, up to 86 Kb. The memory units are each addressed separately with the entire memory structure being read or written to every 0.0202 seconds. This means only one memory address is read per clock cycle to avoid collisions between data being sent out by different memory units. The addresses of the structures are shown in Table 3.2 below. The memory is loaded with equal sections of four different hex memory patterns, 00, FF, 55, and C3. These hex patterns translate to binary 00000000, 11111111, 01010101, and 11000011. These are chosen to determine if the different memory values and patterns are more susceptible to radiation induced SEUs.

In addition to the error check, the memory structure runs a stuck bit check which takes 3 read/write cycles. The stuck bit check first loads the negated memory values into each memory address during one write cycle. Then it checks the memory during the following memory cycle. Then the check reloads the original pattern back into memory. The frequency of the stuck bit check is once every 1021 read cycles, however this can easily be altered or removed if stuck bits do not show up in the data during radiations.

The structure of the DUT board is shown in Figure 3.18. For each memory address, the board outputs the corresponding memory information and checks it with the

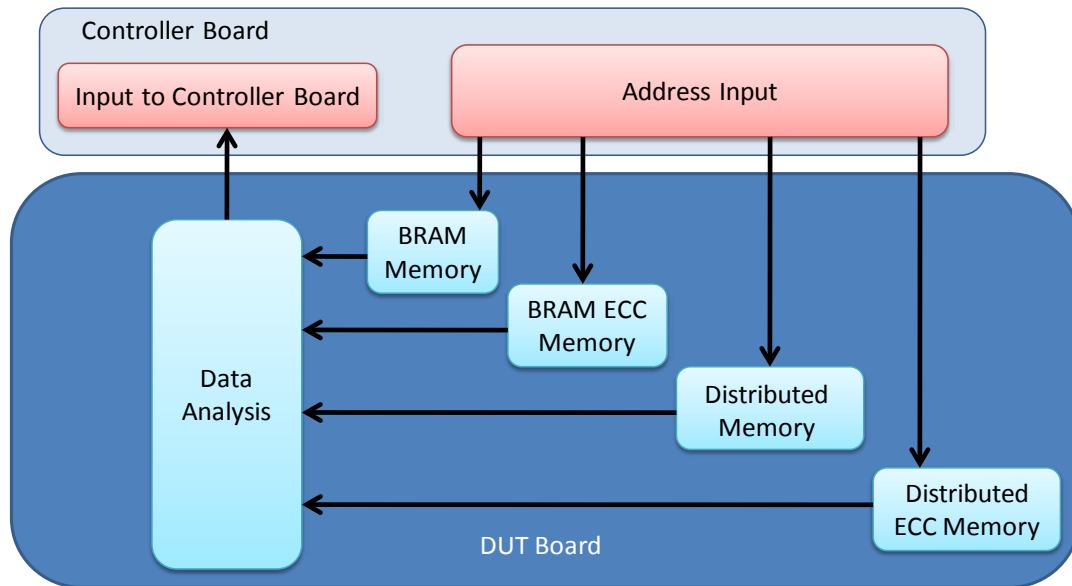


Figure 3.18: Virtex 4 FPGA Memory Structure

expected value for that location. For ECC memories, this means that DUT checks the 13 bit encoded value. Any discrepancies are reported to the controller board as 8 bit data plus the error correction code. For the ECC portion of memory, the data is checked for errors while it is still encoded. Then if there are errors, it is decoded for transmission back to the control board. This is done so that errors that are corrected by the ECC could be seen to evaluate the performance of the ECC. Additionally when errors are detected, the correct value is rewritten into the memory address to attempt to fix the errors.

The controller board software structure combined with this memory DUT software structure contains the logic to take all the memory errors and displays the total number of errors differentiating between the original patterns and the inverted patterns when they are loaded into each section of the memory. Additionally, when an error occurs, the

control board outputs the data with a time stamp based on the DUT clock. However, if errors at multiple addresses occur faster than the data can be captured by the UART running at 9600bps, the actual error is not displayed and only the error count can be used for analysis. This method offers a glimpse at the error data but primarily counts total errors in the memory structure for purpose of analysis. To account for this known system limitation the data is fixed by the DUT when an error is found and the control board records how many single bit and multiple bit errors occurred in each memory structure. Figure 3.19 shows the structure of the control board IP Cores, specifically the test IP core consisting of the VHDL code that captures the data from the DUT.

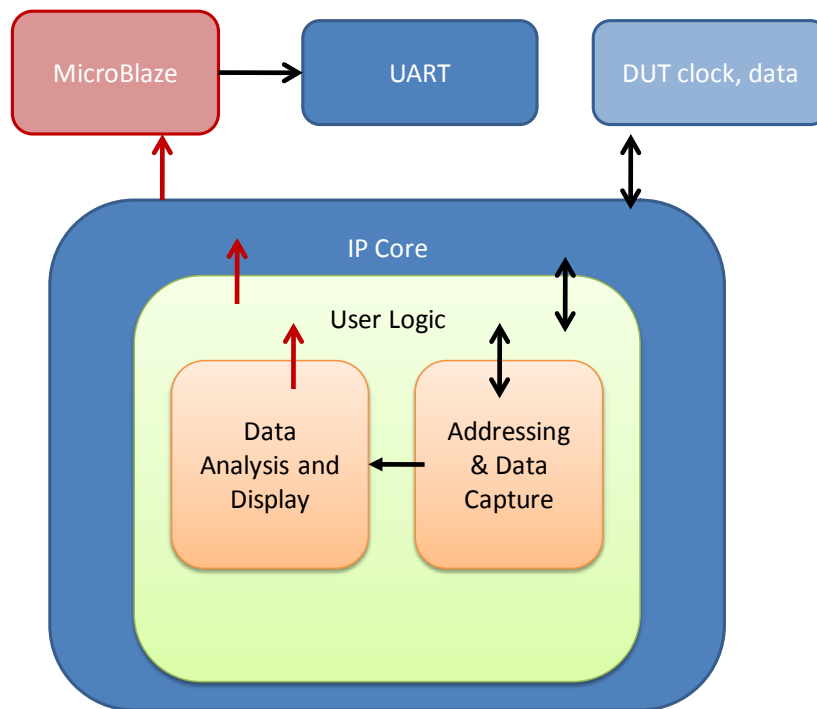


Figure 3.19: Virtex 5 Memory Analysis Structure

Table 3.2: Memory Structure Addresses

Memory Structure	Addresses	Base Address	End Address
BRAM	0-16k	0000000000000000	0011111111111111
BRAM ECC	16-32k	0100000000000000	0111111111111111
Dist. RAM	32-40k	1000000000000000	1001111111111111
Dist. RAM ECC	40-48k	1010000000000000	1011111111111111
BRAM	48-64k	1100000000000000	1111111111111111

3.4 Test Plan

Radiation analysis is conducted on a maximum of 10 FPGA Mini-modules. The initial test is run at 50 krad (Si)/hr dose rate. This dose rate is expected to cause data errors and board failure based on research with previous generations of FPGAs (Wang, Katz and Cronquist). However, since no data is obtained on Virtex 4 FPGAs or the packaged FPGAs such as the Virtex 4 Mini-module, the first radiation determines the radiation dose rates for additional runs. In addition to the error data collected for analysis, current and voltage data is also recorded in order to predict expected errors and device failure on future runs. This ideally allows for devices to be powered off or removed from the source before any permanent damage occurs. The analysis beginning with the FTMR/Adder structure contains the most variety of test structures for analysis. This test compares three designs of adders to a TMR system that votes on the outputs of all three adders. This test shows which designs are the most robust adder designs and shows the performance improvement of both on-chip and off chip FTMR structures. Next, the FTMR/TMR structure is radiated to evaluate the improvements of the FTMR structure compared to traditional TMR structures. Finally, the memory structure tests are

run to evaluate the radiation exposure on a larger portion of the FPGA, as well as, evaluate the improvements of ECC memory over non-ECC memory in both BRAM and distributed memories. These tests are lowest priority since the errors observed by the control board are difficult to trace since the errors could be caused by the additional logic on the DUT that looks like errors in the actual memory addresses tested.

3.4.1 Data Format

The data output from the control board contains data that is used to characterize radiation effects on the various hardening by design techniques. There are two basic formats of data that is output depending on the experiment being run. The first type of data is for the adder and TMR data. The second type of data contains address and data information from the memory system. Both sets of data include a system clock for analysis. All data values are in Hexadecimal, which shorts the size of the output line, thus increasing the amount of data that can be displayed.

The adder TMR data is listed Table 3.3. The data shows each of the four functional units with the current status compared to the truth value of that unit, followed by the error count of the function unit. The functional units are followed by the current status and error counts of the three different types of counter being tested. This data is shorter than the adder TMR data since the counter outputs are not sent to the control board but instead the error code produced by the majority voter on the counters is sent to the control board. Similarly, the data for the FTMR/TMR irradiations contains the four

Table 3.3: TMR Data Collection Format

Example Output Data

```
rcEE#0 behEE#0 claEE#F ftmrEE#0 fcnt#0 clk5DDEF05
rcEE#0 behEE#0 claEE#F ftmrEE#0 cntr0:0:0:0 clk5DDEF05
```

DUT Data sent from each Device

Control Board Truth Data

Cumulative Error Counts for each Device

3.24 MHz Clock Counter

```
rc=    1st Device on DUT
beh=   2nd Device on DUT
cla=   3rd Device on DUT
ftmr=  4th Device on DUT
fcnt=  Control Board TMR voting on Devices 1-3
cntr=  TMR error code output from counter TMR on DUT
```

functional units with outputs displayed in the same format. This is followed by the counter data tested.

The format of the memory software structure includes address, memory data, clock and cumulative errors for each of the four memory types. The cumulative errors are necessary since the serial communication to the PC is limited to 9600 bps and therefore only some data errors is displayed if they are sent to the control board while another error is being displayed.

3.5 Methodology Summary

The system is built to test the radiation effects on the Virtex 4 FPGA. The DUT for this analysis is a Virtex 4 Mini-module. Section 3.2 describes the hardware setup with the control board that provides inputs, analysis and data display to a PC. The two test setups for analysis are described in Section 3.3. They include a memory and ECC

memory setup and a TMR setup. Section 3.4 describes the test plan for the irradiations at OSU NRL.

IV. Results and Analysis

4.1 Chapter Overview

This chapter covers the following material:

1. Radiations Summary
2. Current Draw during Radiation Testing
3. FTMR/TMR/Adder Results
4. Memory Results

The raw data is in Appendix C, while the detailed results of each radiation run is in Appendix D.

4.2 Radiations Summary

The analysis involves eight irradiations. The radiations all use new Virtex 4 Mini-modules which are tested in the lab prior to radiation and operate satisfactorily without producing any errors. Radiation #2 is not complete because the current draw reached the maximum allowed by the Agilent Power Supply and therefore is terminated early. This meant that for the remaining runs a new power supply is used. Radiation #3 also did not produce a total ionizing dose for failure since it is removed while the FPGA DUT is still operating. Figure 4.1 and Table 4.1 summarize the radiation dose rates and time to failure for each run.

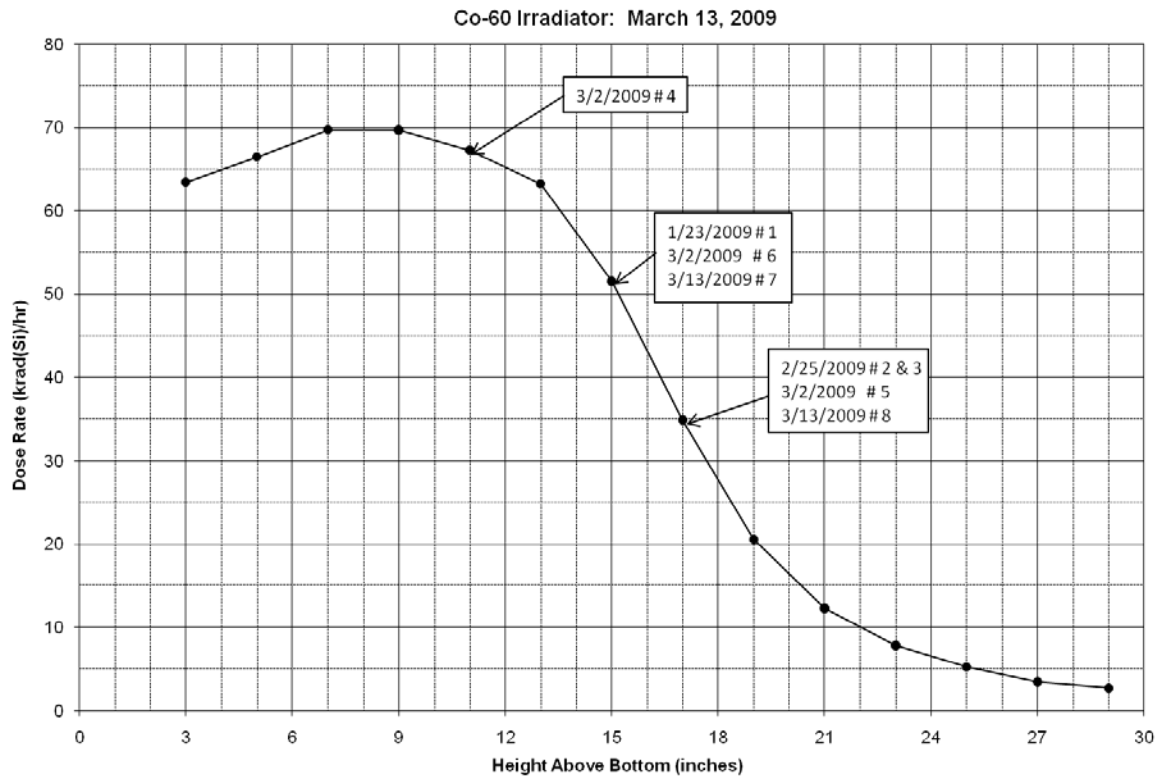


Figure 4.1 Radiations 1-8: Shows krad(Si)/hr vs. Position in Tube

Table 4.1: Summary of Radiations

Radiation #	Dose Rate (krad(Si)/hr)	Radiation Time	Time to Failure	Total Ionizing Dose	Test Run
1	50	0:19:17	0:19:17	16.71	FTMR/Adder
2	35	0:36:30	N/A	21.29	FTMR/Adder
3	35	2:57:24	N/A	103.48	FTMR/Adder
4	67	0:31:02	0:31:02	34.65	FTMR/Adder
5	35	2:42:45	2:42:45	94.94	FTMR/Adder
6	50	1:06:55	1:06:55	57.99	TMR/FTMR

A summary of the different software codes is described in Tables 4.2, 4.3, and 4.4. Table 4.2 shows the code version that is used on each run. Tables 4.3 and 4.4 describe the differences in each code setup used. DUT code version 2.2 included a replacing the 4 bit counter TMR result code with the carryouts from each of the 4 functional units being tested. This is done to get a better understanding of the effects on the whole adder units.

Table 4.2: Software Configurations for each Radiation

Radiation #	Date Tested	Control Board Version	DUT code Version	Outputs of DUT
1	1/23/2009	1	1	FTMR/3 Adders/Cntr TMR
2	2/25/2009	2	2	FTMR/3 Adders/Cntr TMR
3	2/25/2009	2	2	FTMR/3 Adders/Cntr TMR
4	3/2/2009	3	2	FTMR/3 Adders/Cntr TMR
5	3/2/2009	3	2	FTMR/3 Adders/Cntr TMR
6	3/2/2009	3	2.1	FTMR/3 TMRs/Cntr TMR
7	3/13/2009	4	2.2	FMTR/3 Adders
8	3/13/2009	4	2.3	FMTR/CLA Adders

Table 4.3: DUT Code Versions

DUT Code Versions	Outputs	Change
1	CLA, Behavioral, RC, FTMR	Original Code
2	CLA, Behavioral, RC, FTMR, Counter TMR data	Major modifications of communication between boards
2.1	3 TMRs(CLA, Behavioral, RC), FTMR, Counter TMR data	Outputs to I/O Pins
2.2	CLA, Behavioral, RC, FTMR	counter TMR data replaced by Carry outs of adders and FTMR
2.3	3 CLA Adders, FTMR	Outputs to I/O Pins

Table 4.4: Control Board Code Versions

Control Code Version	Change
1	Original working code
2	Change communication between boards to make it into a robust design without errors and added counter TMR to additional output lines
3	Minor modifications to output format to include regular clock updates at 10 sec intervals and error counts at 2 min intervals
4	Setup to receive and compare 5 bit inputs from DUT, also analyzes data in a control board TMR

The results of the radiations indicate that the total ionizing dose to cause device failure on the Virtex 4 Mini-modules is difficult to predict. In fact the largest dose rate in Radiation #4 experienced failure at nearly twice the total ionizing dose that caused radiation #1 to fail. This is likely the result of the code revision done after radiation #1 but could also be a result of variations in the modules that are used for analysis. Additionally, these variations could be the result of variations in placement of the device within the gamma irradiator itself. The position could only be controlled in the vertical axis but the actual rotation of the device in the gamma cell is not controllable. Therefore, an analysis of current draw versus device failure and SEUs is shown in Section 4.3.

4.3 Current Draw

The current draw of the FPGAs indicates the amount that leakage current in the FPGA increases due to the EHPs described in Section 2. It indicates when SEU might cause incorrect values to be recorded. This current is used to determine at what point an SEB would be expected to permanently damage the device under radiation. Figures 4.2 and 4.3 show the current during each irradiation for all 6 radiations. These tables are divided between the 35 krad (Si)/hr radiations and the higher dose rates, so that trends are easily observed.

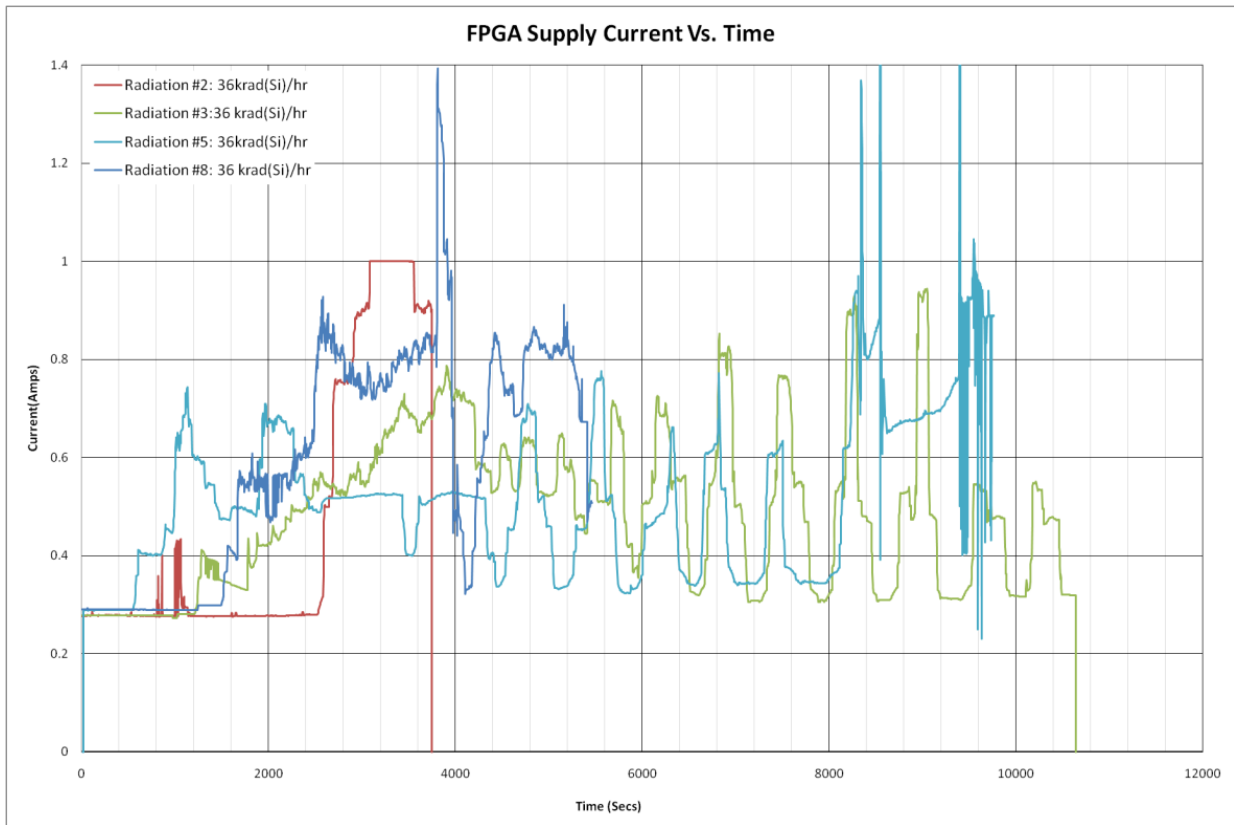


Figure 4.2: FPGA Supply Current vs. Time at 35 krad (Si)/hr

Figure 4.2 shows similar current draw for 35 krad (Si)/hr radiations. Both Radiations 5 and 8 experienced enough radiation effects to experience device failure. As discussed above radiation 2 and 3 did not result in device failure before the DUT is removed from radiation. However, the devices did not experience similar maximum currents prior to shutdown as expected from Wang et al discussed in Chapter 2. Based on these results, it is difficult, if not impossible, to determine device failure based on current draw alone. One explanation for this result is the fact that the FPGA is integrated into the device unlike previous FPGAs which are plugged into integrated circuit sockets.

Therefore the current analysis may reveal more consistent results prior to failure by measuring the three FPGA power supplies (1.2V, 2.5V and 3.3V) as they connect directly to the FPGA as opposed to the current draw through the constant voltage 5 V power supply which is measured.

Figure 4.3 shows the currents of the three higher radiations. As discussed in Chapter 3, the expected dose rate for maximum errors is not known prior to testing. Therefore, radiation 1 is used as a baseline. However, after the device used in Radiation #3 did not fail and produced limited SEU errors after nearly 3 hours with a dose rate of 35 krad compared to the 50 krad of Radiation #1, a higher radiation dose rate is used in Radiation #4. Thus Radiation #4 resulted in device failure faster than expected.

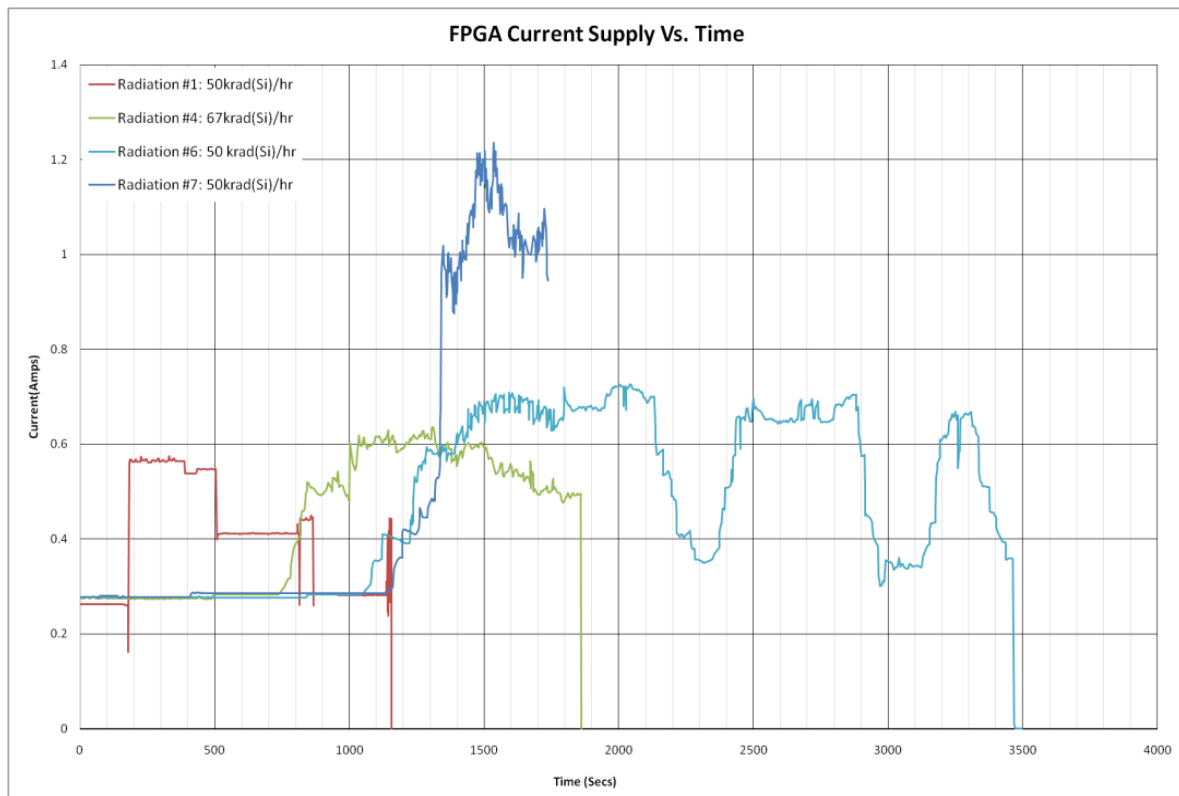


Figure 4.3: Supply Current Vs Time at 50 krad (Si)/hr and 67 krad (Si)/hr

Radiation #6 is conducted to re-evaluate the 50 krad (Si)/hour dose rate and showed that some other effects is occurring in Radiation #1 that didn't occur in the other radiation. Therefore, for the analysis, Radiation #1 data is being considered incomplete and Radiations #4 and #6 are assumed to be the estimated radiation TID for failure. Radiation #7 also did not experience TID failure and therefore it is also being excluded for this purpose.

4.4 FTMR/Adder Error Results

FTMR and each functional adders error results are in the Table 4.5. The data shows that the FTMR circuit experienced the most errors at the output of the DUT. This result is initially surprising based on the expected improvements of a TMR circuit over a single copy of a circuit. However, when analyzing the device utilization of each component, the FTMR circuit utilization is higher than any of the adders by themselves. Based on the results of the above test, an analysis of using traditional TMR designs of the 3 different functional units is done. This implementation is done to verify whether a single copy TMR design can outperforms the FTMR. The TMRs were based on using 3 identical copies for each TMR. FTMR vs. TMR analysis error results are in the Table 4.6.

Table 4.4: Single Adder vs. Single FTMR Errors (* partial radiations)

Radiation #	Dose Rate (krad(Si)/hr)	RC Adder Errors	Behavioral Adder Errors	CLA Adder Errors	FTMR Errors
2*	35	0	0	0	1
3*	35	0	0	1	3900
4	67	4260	0	6124	6657
5	35	1160759	1454061	1618623	1532825

Table 4.5: TMR vs. FTMR Errors

Radiation #	Dose Rate(krad(Si)/hr)	RC TMR Errors	Behavioral TMR Errors	CLA TMR Errors	FTMR Errors
6	50	6293004	4763530	5354154	4763530

The results of comparing various TMR units with single triplicated functional units reveal that the FTMR design can produce results worse than the simple single functional unit TMRs. This indicates that the likelihood of errors on any functional component increases proportionally to other functional units. Therefore, these results indicate that an FTMR circuit does not produce increased protection as hypothesized in Chapter 3.

For further analysis of the data, the cumulative errors over time for radiation # 4, 5, & 6 are shown in Figures 4.4, 4.5, and 4.6. These figures show the errors just prior to device failure since the errors prior to this point are extremely rare and appear to vary randomly when compared to the results produced as the FPGA reaches its failure point. These graphs end when either the clock signal stopped transmitting to the control board or where the correct results being output to the controller board stopped being sent for an entire display cycle through the serial communication.

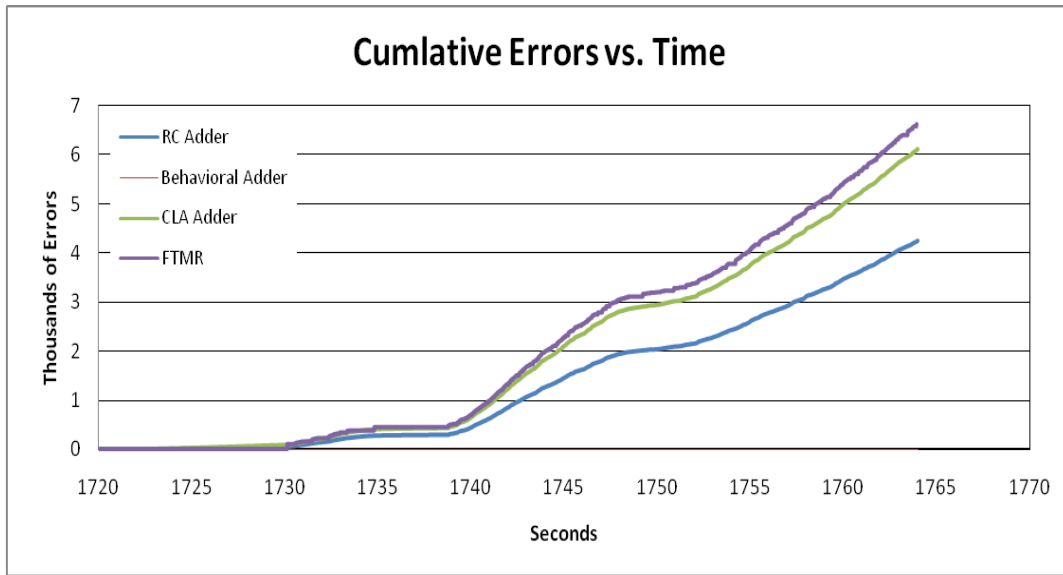


Figure 4.4 Errors on Radiation #4 67krad (Si)/hr

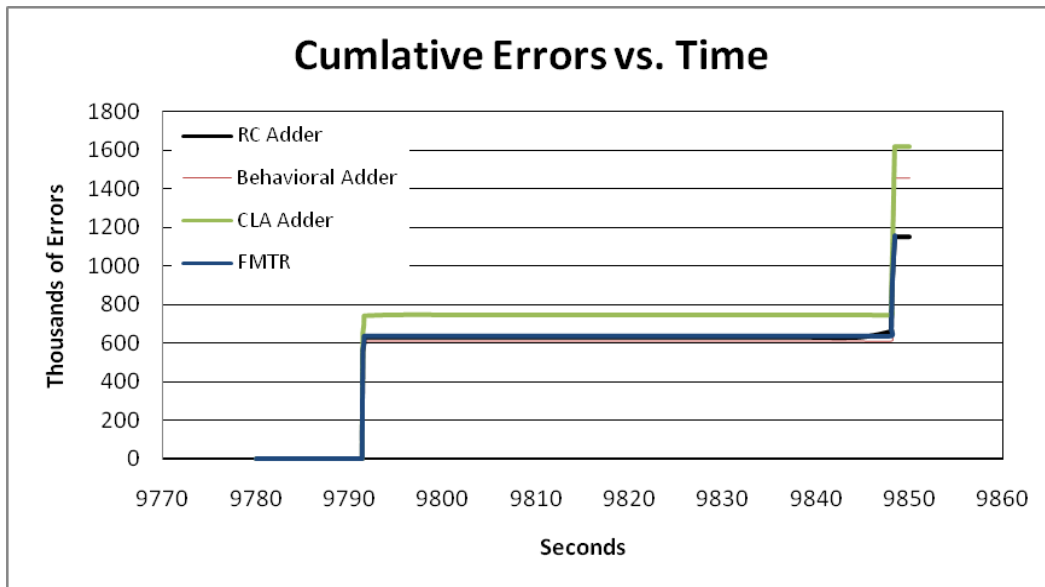


Figure 4.5: Error on Radiation #5 35 krad (Si)/hr

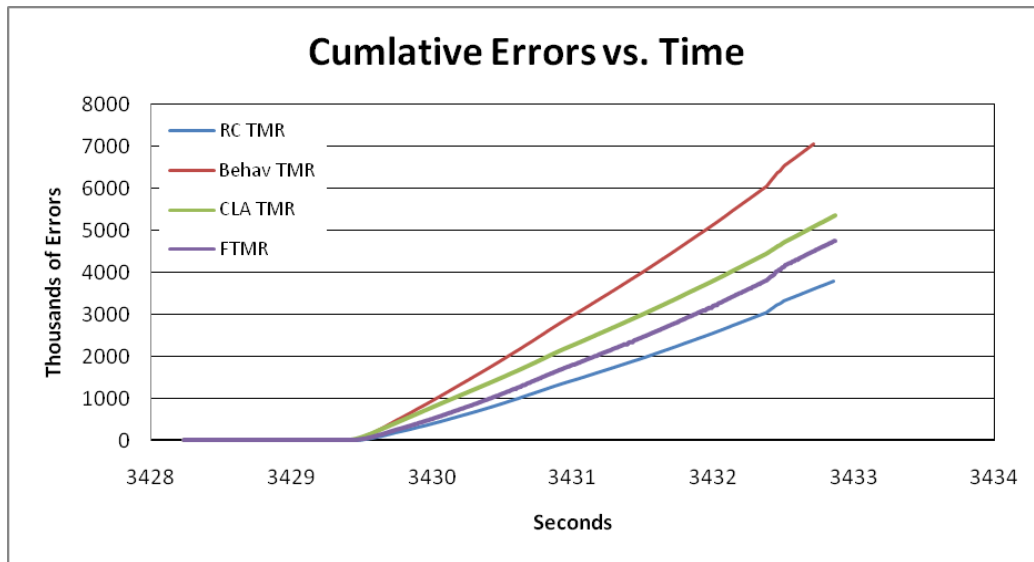


Figure 4.6: Errors on Radiation#6 50 krad (Si)/hr

These three figures show the majority of errors just prior to device failure. This results in a major limitation of this type of testing. In fact less than 1000 total errors, across all functional units, occur prior to the minute before device failure on all 8 radiations.

Additional analysis of the results indicates that the ripple carry adder has the best performance of the three types of adders analyzed. This result was actually better than the result of the single voter FTMR implemented.

4.6 Results Summary

The results show the single voter FTMR device does not perform as well as traditional TMR circuits built with single copies of more robust adders. This shows that the cycles that have error occurrences on different functional units has less to do with structure and more to do with the EHP in the individual structures. Additionally, the

FTMR circuit performed worse than single devices outputting data to the control board in almost all cases. However, when the FTMR is moved off chip, the results are significantly improved. This indicates that the single point of failure of a TMR circuit should be mitigated by one of the techniques discussed in Chapter 2.

V. Conclusions

5.1 Overview

This chapter covers the following material:

1. A basic conclusion statement
2. Applications
3. Future Studies

5.2 Conclusion Statement

Radiation effects produces SEUs and device failure in Virtex 4 Mini-modules allowing characterization of the hardened by design components. Single Voter TMR and FTMR structures placed on the DUT experiences error rates as large as the single units tested.

5.3 Applications

The results show single voter TMR designs do not necessarily improve design hardness when the TMR design is also radiated. The TMRs placed after three functionally different combinational adders actually had worse performance results than that of the behavioral adder that Xilinx defaults to. These results are mainly caused by the differences in device structure causing more space to be utilized and therefore more errors to be produced.

5.4 Future Work

Possible areas of future study include analysis of more advanced hardening design techniques such as those discussed in Chapters 2 and 3. These techniques for TMR include using word-wise TMR voting or developing a buffer based TMR implementation. Alternatively, more robust modularly redundant designs could be proposed that would limit the effects of SEUs on the FPGAs.

Another possible area of study is to compare varying module sizes between triplicated TMRs. This could be used to optimize the placement of voting logic to maximize error protection while minimizing additional size overhead caused by the voting logic.

Additionally, further development of this testing methodology could be done to eliminate possible errors that could have occurred based on the stress placed on the clock signals. This would require significant numbers of tests to evaluate performance of the FPGA boards in the radiation environments.

Finally, these structures could be implemented as gate level devices across multiple slices in the FPGA. This would increase the FPGA utilization size and potentially will allow analysis of error locations by analyzing the signals in between the individual slices

Bibliography

- Ames, B. "New technologies drive bulk-memory solutions." Military & Aerospace Electronics 2003.
- Arnold, D.M. Enhancing Residual Memory Effects of Dynamic Random Access Memory (DRAM) Using Gamma Radiation. Air Force Institute of Technology:. Wright-Patterson AFB, OH. , 2008,.
- Brown, W. D. and J. E. Brewer. Nonvolatile Semiconductor Memory Technology. Piscataway, New Jersey: IEEE Press, 1998.
- Bushnell, M. L. and V. D. Agrawal. Essentials of electronic testing for digital, memory, and mixed-signal VLSI circuits. Frontiers in electronic testing. Boston: Kluwer Academic, 2000.
- Ceschia, M, et al. "Identification and Classification of Single Event Upsets in the Configuration Memory of SRAM-based FPGAs." IEEE Transactions on Nuclear Science 50.6 (2003): 2088-2094.
- Claeys, C. and E. Simoen. Radiation Effects in Advanced Semiconductor Materials and Devices. Berlin: Springer-Verlag, 2002.
- Gusmao, Fernanda, et al. "Designing Fault-Tolerant Techniques for SRAM-based FPGAs." IEEE Design and Test of Computers (2004): 552-556.
- Herminghuysen, Kevin. OSU NRL Co-60 Curve. Excel Spreadsheet. Jan 2002.
- Xilinx Wesite, Inc., Xilinx. 2009. <www.xilinx.com>.
- Karl, Mohr, Giby Samson and Lawrence Clark. "A Radiation Hardened by Design Register file with Lightweight Error Detection and Correction." IEEE Transactions on Nuclear Science 54.4 (2007): 1335-1340.
- Lam E. "Enhancing Residual Memory Effects of Dynamic Random Access Memory (DRAM) Using Gamma Radiation." Air Force Institute of Technology: Wright-Patterson AFB, OH. (2008): p. 76.
- Normand, Eugene. "Single Event Upset at Ground Level." IEEE Transactions on Nuclear Science 43.6 (1996): 2742-2744.

Petrosky, James. Radiation Effects on Electronic Devices: Theory, Modeling and Experiment. NENG660 Course Notes. Air Force Institute of Technology, 2007., n.d.

Radiation Effects & Analysis Home Page. 2008. 27 05 2008
<<http://radhome.gsfc.nasa.gov>>.

Rollins, Nathan, et al. "Evaluating TMR Techniques in the Presence of Single Event Upsets." 2003.

Sinclair, R. Beech, R. "High Speed, Radiation Hard MRAM Buffer." Non-Volatile Memory Technology Symposium (November 4 - 6, 2002): 6.

Wang, JJ, et al. "SRAM Based Re-programmable FPGA for Space Applications." IEEE Transactions on Nuclear Science 46.6 (1999): 1728-1732.

APPENDIX A

Wiring Structure on CD

APPENDIX B

Code on CD

APPENDIX C

Raw Data on CD

APPENDIX D

Detailed Results on CD

REPORT DOCUMENTATION PAGE				Form Approved OMB No. 0704-0188	
<p>The public reporting burden for this collection of information is estimated to average 1 hour per response, including the time for reviewing instructions, searching existing data sources, gathering and maintaining the data needed, and completing and reviewing the collection of information. Send comments regarding this burden estimate or any other aspect of this collection of information, including suggestions for reducing this burden to Department of Defense, Washington Headquarters Services, Directorate for Information Operations and Reports (0704-0188), 1215 Jefferson Davis Highway, Suite 1204, Arlington, VA 22202-4302. Respondents should be aware that notwithstanding any other provision of law, no person shall be subject to any penalty for failing to comply with a collection of information if it does not display a currently valid OMB control number. PLEASE DO NOT RETURN YOUR FORM TO THE ABOVE ADDRESS.</p>					
1. REPORT DATE (DD-MM-YYYY)		2. REPORT TYPE		3. DATES COVERED (From — To)	
26-03-2009		Master's Thesis		Jun 2007 — Mar 2009	
4. TITLE AND SUBTITLE CHARACTERIZATION OF HARDENING BY DESIGN TECHNIQUES ON COMMERCIAL, SMALL FEATURE SIZED FIELD-PROGRAMMABLE GATE ARRAYS				5a. CONTRACT NUMBER	
				5b. GRANT NUMBER	
				5c. PROGRAM ELEMENT NUMBER	
6. AUTHOR(S) Thomas E. Simmons, Capt, USAF				5d. PROJECT NUMBER	
				08-183	
				5e. TASK NUMBER	
				5f. WORK UNIT NUMBER	
7. PERFORMING ORGANIZATION NAME(S) AND ADDRESS(ES) Air Force Institute of Technology Graduate School of Engineering and Management (AFIT/EN) 2950 Hobson Way WPAFB OH 45433-7765				8. PERFORMING ORGANIZATION REPORT NUMBER AFIT/GE/ENG/09-43	
9. SPONSORING / MONITORING AGENCY NAME(S) AND ADDRESS(ES) Air Force Research Laboratory/Space Vehicles ATTN: Dr. James Lyke 3550 Aberdeen Ave SE, Bldg 887 Rm 3 Kirtland AFB, NM 87117 (505) 846-5812 DSN 246-5812				10. SPONSOR/MONITOR'S ACRONYM(S) AFRL/RVSE	
				11. SPONSOR/MONITOR'S REPORT NUMBER(S)	
12. DISTRIBUTION / AVAILABILITY STATEMENT Approval for public release; distribution is unlimited.					
13. SUPPLEMENTARY NOTES					
14. ABSTRACT This thesis experimentally tests and evaluates programmable logic devices under gamma irradiation to determine radiation effects and characterize improvements of various hardening by design techniques - Error Correction Coding (ECC) and Triple Modular Redundancy (TMR). The TMR circuit includes three different functional implementations of adders compared to TMR voted circuits of those same adders. The TMR is implemented with the same functional adders and as a Functional TMR (FTMR) with three different function adders that are voted on. These adders are connected to single voter TMR and FTMR circuits to evaluate the improvements. The circuit is designed to check for errors in memory data, stuck bit values in the memory, and the performance improvements that ECC provides the system. The results show that TMR or FTMR circuits failed at a rate at or above the single copy adders. This results from the single point of failure created by the voting logic in the radiation environment. When the TMR or FTMR circuit is moved off-chip, the TMR single point of failure is removed and the results demonstrate much lower SEU error rates.					
15. SUBJECT TERMS Irradiation, Gamma Radiation, Computer Architecture, Computers, Chips (Electronics)					
16. SECURITY CLASSIFICATION OF:			17. LIMITATION OF ABSTRACT	18. NUMBER OF PAGES	19a. NAME OF RESPONSIBLE PERSON
a. REPORT	b. ABSTRACT	c. THIS PAGE			Dr. Yong C. Kim
U	U	U	UU	68	19b. TELEPHONE NUMBER (include area code) 937-255-3636, ext 4620; yong.kim@afit.edu